Late Middle Pleistocene hominin teeth from Panxian Dadong, South China

Wu Liu [a,*], Lynne A. Schepartz [a,b], Song Xing [a,c], Sari Miller-Antonio [d], Xiujie Wu [a], Erik Trinkaus [e], María Martinón-Torres [f,**]

[a] Key Laboratory of Vertebrate Evolution and Human Origin of Chinese Academy of Sciences, Institute of Vertebrate Paleontology and Paleoanthropology, Chinese Academy of Sciences, Beijing 100044, China
[b] School of Anatomical Sciences, University of the Witwatersrand Medical School, Johannesburg, South Africa
[c] Graduate School of the Chinese Academy of Sciences, Beijing 100049, China
[d] Department of Anthropology, Geography and Ethnic Studies, California State University at Stanislaus, Turlock CA, USA
[e] Department of Anthropology, Washington University, Saint Louis, MO 63130, USA
[f] Centro Nacional de Investigación sobre la Evolución Humana (CENIEH), Burgos, Spain

ABSTRACT

The hominin teeth and evidence of hominin activities recovered from 1991 to 2005 at the Panxian Dadong site in South China are dated to the late Middle Pleistocene (MIS 8–6 or ca. 130–300 ka), a period for which very little is known about the morphology of Asian populations. The present study provides the first detailed morphometric description and comparisons of four hominin teeth (I^1, C_1, P^3 and P_3) from this site. Our study shows that the Panxian Dadong teeth combine archaic and derived features that align them with Middle and Upper Pleistocene fossils from East and West Asia and Europe. These teeth do not display any typical Neanderthal features and they are generally more derived than other contemporaneous populations from Asia and Africa. However, the derived traits are not diagnostic enough to specifically link the Panxian Dadong teeth to *Homo sapiens*, a common problem when analyzing the Middle Pleistocene dental record from Africa and Asia. These findings are contextualized in the discussion of the evolutionary course of Asian Middle Pleistocene hominins, and they highlight the necessity of incorporating the Asian fossil record in the still open debate about the origin of *H. sapiens*.

© 2013 Elsevier Ltd. All rights reserved.

Introduction

For the past two decades, research and debates on modern human origins have focused on the emergence of anatomically modern humans (AMHS) around the world. Some recent fossil discoveries are interpreted as evidence that early modern humans appeared in East Africa by 160 ka or even earlier (White et al., 2003; McDougall et al., 2005). In East Asia, because of the paucity of fossil discoveries and unreliable dating, it has long been argued that early AMHS did not appear until 50 ka (Shang et al., 2007). Recently, studies of new Upper Pleistocene hominin fossils from the Huanglong and Zhiren caves suggest that early AMHS may have been present in East Asia as early as 100 ka (Liu et al., 2010a, b). In addition, a recent analysis of a Middle Pleistocene

dental assemblage from Qesem Cave (Israel) leaves open the possibility that this non-African population may belong to early *Homo sapiens* (Hershkovitz et al., 2011). In this context, the phylogenetic and taxonomic assessments of the Middle Pleistocene lineages preceding the appearance of *H. sapiens* have become a crucial piece in the debate about the origins of modern humans. Although a relatively large number of late Middle Pleistocene hominins have been found in East Asia (Wu and Poirier, 1995; Etler, 1996), these fossils have not been consistently included in current debates about the origin of AMHS, and little is known about their phylogenetic place in relation to contemporary hominins from Africa and Europe as well as to Upper Pleistocene hominins. This study presents a detailed description and comparative analysis of four hominin teeth recovered from the late Middle Pleistocene cave site of Panxian Dadong (PD), Guizhou of South China, including two new teeth recovered in 1998–2000 and the reassessment of two teeth already described (Liu and Si, 1997). The morphological and metric comparison of these four teeth will be contextualized in the discussion about the evolutionary course of the Middle Pleistocene of Asia.

* Corresponding author.
** Corresponding author.
   E-mail addresses: liuwu@ivpp.ac.cn (W. Liu), maria.martinon.torres@gmail.com (M. Martinón-Torres).

The site

Panxian Dadong Cave, located in Guizhou Province, south-western China (25°37′38″N, 104°8′44″E; Fig. 1), is part of a large karst system that contains three connected stacked caves. The present elevation of the middle chamber, 230 m above the valley floor, is in part the result of Middle Pleistocene uplift associated with the Qinghai-Xizang (Tibetan Plateau). This large cavern is 250 m deep, between 23 and 56 m wide at various points, and has a vaulted ceiling ranging in height from 22 to 30 m. In 1990, mammalian fossils and stone artifacts were first found in the cave. From 1992 to 2005, a collaborative international team of scientists headed by the Institute of Vertebrate Paleontology and Paleoanthropology conducted several seasons of excavations that yielded four hominin teeth and a lithic assemblage associated with an *Ailuropoda–Stegodon* fauna. Additional evidence of hominin activities in the cave consists of cut-marked and burnt bone (Schepartz and Miller-Antonio, 2010). Faunal comparisons, Uranium-series (U-series) dates of speleothems (Shen et al., 1997), and electron spin resonance (ESR) dates on tooth enamel (Rink et al., 2003; Jones et al., 2004) indicate that most of the excavated levels at Dadong were deposited between MIS 8 and MIS 6 (130–300 ka; Huang et al., 1995; Huang and Hou, 1997; Jones et al., 2004; Schepartz and Miller-Antonio, 2004).

For more than twenty years, multidisciplinary studies of the lithics, fauna, cave deposits, and chronological correlations were conducted. The results confirm that Panxian Dadong contains an extensive record of late Middle Pleistocene human activities involving behavioral flexibility and unique adaptations to a mountainous environment. The lithic analyses, that focused on raw material type, differential use of materials, and technological characteristics, show that prepared core (Levallois-like) flaking techniques are present (Huang and Hou, 1997) and also that some aspects of tool production changed through time. For example, limestone artifacts dominate the assemblage but they are the least reworked component. By contrast, chert is used most intensively for retouched tools and basalt is mostly fashioned into simple flakes. The latter two materials are found with greater frequency in the upper levels of the deposits. The differential distribution suggests a shift in raw material use over a relatively short period of time – approximately 100,000 years (Miller-Antonio et al., 2004; Paraso et al., 2006). This may be interpreted as an adaptive

response to climatic fluctuations since the microstratigraphic studies of the cave deposits have identified freeze-thaw features that signal very cold and unusually wet glacial periods (Karkanas et al., 2008).

The paleoenvironmental interpretation of the depositional sequence, based on geomorphology and microstratigraphic studies, indicates that most of the archaeological levels accumulated during glacial times and therefore, the cave was most heavily used by hominins during these cold, wet intervals. The fauna indicates that a mixed woodland environment prevailed; this included bamboo forests (*Ailuropoda* habitat) and open rocky areas with abundant grasses. Species representation through time is very consistent, and the most prevalent animals are highly adaptable forms with broad environmental ranges such as stegodonts and rhinoceros. Carnivores are not well represented, and there is little evidence that they were an important taphonomic agent in the formation of the assemblage. Moreover, detailed analyses of the stegodont and rhinoceros samples produced age-at-death profiles that show differential representation of certain age groups rather than natural mortality patterns. The *Rhinoceros sinensis* dental eruption and tooth wear data document the predominance of prime age adults (Schepartz and Miller-Antonio, 2010). By contrast, the dental remains of *Stegodon orientalis* indicate an over-representation of younger animals, 0–12 yrs (Schepartz et al., 2001, 2005). This comparative faunal research supports the interpretation that hominins are the primary agent of faunal accumulation in Dadong and therefore may have been responsible for the relative consistency of the assemblage over time. It also appears that hominins were probably not present during interglacial periods, and that carnivore use of the cave did not increase during their absences, as has been documented for many Palaeolithic cave sites (c.f., Stiner, 1994, 2004; Rabinovich and Hovers, 2004; Diedrich, 2010). One explanation might be that the denser subtropical forests of the interglacial could have resulted in lower prey densities of the large animals such as stegodonts, rhinoceros, bovids and cervids.

Two volumes of collected papers on the Panxian Dadong excavations were published in 1997 and 2004 respectively (Huang, 1997; Schepartz and Miller-Antonio, 2004). In the 1997 volume, two hominin teeth found in earlier explorations of the cave were described (Liu and Si, 1997). Two additional teeth were discovered in 1998 and 2000. In recent years, the Middle and Upper Pleistocene fossil and archaeological record in China and worldwide has

Figure 1. Geographic location and view of the entrance to Panxian Dadong.

dramatically increased. It is now possible to conduct a broader comparative study of the Panxian Dadong hominin teeth to further inform our understanding of late Middle Pleistocene hominin evolution in East Asia.

Materials and methods

Materials

Four hominin teeth from Panxian Dadong, including an upper central incisor (I^1), a lower canine (C_1), an upper third premolar (P^3) and lower third premolar (P_3), are described and analyzed in the current study. The teeth were found during the field seasons of 1993–2000 (see Fig. 2). Two of them (I^1 and C_1) have been previously described (Liu and Si, 1997).

We compare the Panxian Dadong teeth with a range of Middle and Upper Pleistocene hominins of Africa, Asia and Europe (Table 1). In order to examine East Asian dental evolutionary trends, we focus on the comparison with several Chinese samples from early Middle Pleistocene, late Middle Pleistocene, Upper Pleistocene, and more recent prehistoric and modern human collections. In the southern and adjacent regions of the Yangtze River in China, Middle and Upper Pleistocene hominin fossils have been found in several sites (Wu and Poirier, 1995; Liu et al., 2010a, b). In previous studies, the specimens from the Upper Pleistocene were usually classified into anatomically modern humans, and earlier dated specimens from the late Middle Pleistocene were regarded as archaic H. sapiens. Some Chinese hominin fossils with similar ages to Panxian Dadong, including Chaoxian, Tongzi, Maba and Changyang, were all classified into archaic H. sapiens. Given the
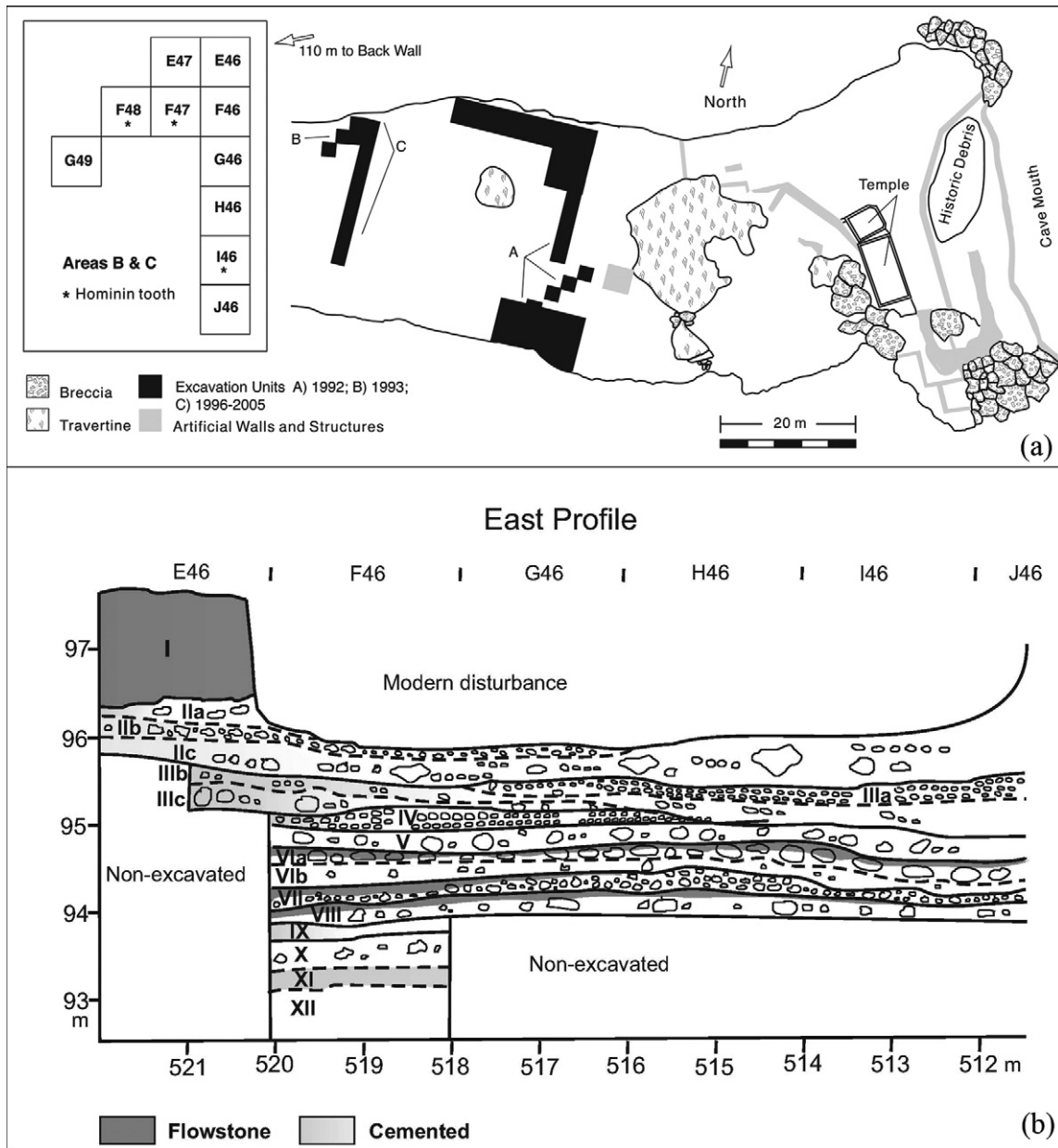

Figure 2. Plan view of the Panxian Dadong excavation area (a). PDH2, PDH3 and PDH4 came from the excavated areas marked in black. PDH1 was found 120 m west of the excavation area where the other teeth were found, and is not shown in this figure. East stratigraphic profile of the excavation in Area C (b). The P^3 is correlated with dated mammalian tooth samples from Layers II–IV that are broadly attributed to glacial MIS 6, while the P_3 is correlated with dated tooth samples from older Layers VI and VII that mark the beginning of interglacial MIS 7 and the termination of glacial MIS 8 (Karkanas et al., 2008).

Table 1
Specimens used for morphological comparisons in present study.[a]

Geography and chronology	Specimens	Resources
China		
Early Pleistocene (~1.0–1.15 mya)	O: Jianshi, Lantian	Collections housed at IVPP
Mid-Middle Pleistocene (~0.7–0.3 mya)	C: Zhoukoudian (ZKD) O: ZKD PA110, PA68; Xichuan, Hexian, Yunxian, Yiyuan	Weidenreich (1937), Liu (1999), Collections housed at IVPP
Late Middle Pleistocene (~0.3–0.12 mya)	O: Changyang, Chaoxian, Tongzi, Xujiayao, Dingcun C: Jinniushan	Collections housed at IVPP, He (2000)
Upper Pleistocene (~110–10 kya)	C: ZKD Upper Cave O: Liujiang, Tubo, Qingliu, Huanglong Cave	Liu (1999), Collections housed at IVPP
Modern humans	O: Neolithic, Bronze Age, recent Chinese	Collections housed at IVPP, Brace (1976, 1984)
West Asia		
Late Middle Pleistocene	Qesem	Hershkovitz et al. (2011)
Upper Pleistocene	Skhul, Qafzeh	Wolpoff (1971), Vandermeersch (1981)
Africa		
Early Pleistocene	O: KNM-WT 15000	
Middle Pleistocene	Tighennif, Rabat, Thomas' Quarry, Jebel Irhoud	Hershkovitz et al. (2011), Bermúdez de Castro et al. (2008), Hublin and Tillier (1981), Ennouchi (1976), Thoma and Vallois (1977)
Europe		
Early Pleistocene	Atapuerca TD6	Bermúdez de Castro (1993), Bermúdez de Castro et al. (1999)
Middle Pleistocene	Atapuerca SH, Mauer	Bermúdez de Castro (1993), Bermúdez de Castro and Nicolas (1995), Bermúdez de Castro et al. (2004), Martinón-Torres et al. (2012)
Neanderthals	Arcy II, Chateauneuf, Ehringsdorf, Genay, Spy, Le Moustier, Tabun, Krapina, Lazaret, l'Hortus, La Quina 5, Monsempron, Ochoz, Valdegoba	Bermúdez de Castro (1993), Bermúdez de Castro and Nicolás (1995), Bermúdez de Castro et al. (2004), Wolpoff (1979)
Upper Pleistocene/Holocene recent humans	O: Dolni Vestonice, Pavlov, medieval collection of San Nicolás (Murcia, Spain), Canary Islanders, Mesolithic French sample (Téviec and Hoëdic), Neolithic French sample (Avize, Dolmens de Bretons, Caverne de L'Homme Mort, Orrouy)	

[a] Data were collected by authors except where noted. O: original fossil, C: cast.

considerable debate about the taxonomic classification of the Middle and Upper Pleistocene fossils in general, we have grouped the comparative specimens into geographical and chronological samples rather than separate taxa, with the exception of Neanderthal specimens. The reason for treating Neanderthals as a separate group is because, on dental grounds, their uniqueness is generally well-recognized (Bailey, 2000, 2002; Martinón-Torres et al., 2007, 2012). Treating them as a separate group in this analysis simplifies the nomenclature for the Upper Pleistocene fossils with which they chronologically overlap and whose taxonomic assignment to the *H. sapiens* lineage is still a matter of debate.

Methods

Tooth wear stages are determined following Molnar (1971). The dental morphology descriptions and comparisons were conducted following the terminology employed in Weidenreich (1937), Bermúdez de Castro (1988), and Martinón-Torres et al. (2008). Some non-metric features were scored using the Arizona State University Dental Anthropology System (ASUDAS; Scott and Turner, 1997). Crummett's classification (1994) was employed for the tuberculum dentale expression.

Mesiodistal (MD) and buccolingual (BL) dimensions of the crown and the root (at the cemento-enamel junction, CEJ), as well as root length (from CEJ to root tip at buccal side) were taken with a standard sliding caliper and recorded to the nearest 0.1 mm following the methods of Flechier, Lefêvre and Verdéne (Lefêvre, 1973; see also Martinón-Torres et al., 2008). Table 2 lists the fossils and samples whose MD and BL diameters were employed for the metric comparison of the PD sample. In order to graphically compare the PD dimensions with the range of variation of each comparative sample we provide a boxplot for each measure. Each boxplot provides the median, the interquartile range, the outliers and the extreme values of a given distribution. Given the nature of the PD

sample, composed of isolated teeth that cannot be assigned to the same individual, further statistical comparisons were not possible.

Geometric morphometric (GM) analysis

GM analysis was conducted on the P^3 and P_3 to examine their crown outline shapes and patterns of cusp arrangement by using standardized pictures of occlusal surfaces. Images were taken with a Cannon 5D digital camera fitted with a 100 mm lens. The camera was fixed to a Kaiser Copy Stand 5510. An aperture of f/32 was used for a maximum depth of field. The distance between the lens and each occlusal surface was constant, with the center focus of the camera being automatically situated on the occlusal surface. Each tooth was photographed with its cemento-enamel junction maximally parallel to the camera lens (Martinón-Torres et al., 2006; Gómez-Robles et al., 2007, 2008, 2011), and a millimeter scale was placed at about the same plane as the occlusal surface. When both antimeres were present, only the same side as that represented at Panxian Dadong was chosen. If only one antimere was preserved in an individual, the tooth was mirrored using Adobe Photoshop®.

The comparative samples include Middle and Upper Pleistocene hominins from Asia, as well as Europe and Africa. In order to explore the polarity of the observed morphologies, some earlier hominins and recent humans are also included (Table 3).

Geometric morphometrics is a method that quantitatively analyzes the shape differences among specimens based on landmark coordinate data (Adams et al., 2004; Zelditch et al., 2004). Through translation, scaling, and rotation (superimposition) it eliminates non-shape elements (such as position, size, and orientation) and retains all of geometric information for further exploration of shape differences (Zelditch et al., 2004; Slice, 2005). Non-uniform components of shape change or disproportional deformation between different shapes can be used to generate a set of shape variables, or partial warp scores (Bookstein, 1989, 1991; Zelditch et al., 2004).

Table 2
List of fossils and samples whose MD and BL diameters were employed for the metric comparison of Panxian Dadong.

Region and chronology	Specimens	References
Africa		
Early Pleistocene	Olduvai, Swartkrans, KNM-ER	Tobias (1991), Wolpoff (1971), Kimbel et al. (2004)
Middle Pleistocene North Africa	Rabat, Tighennif, Thomas' Quarry, Jebel Irhoud	Bermúdez de Castro et al. (2008), Ennouchi (1976), Thoma and Vallois (1977), Hublin and Tillier (1981)
East Asia		
Early Pleistocene (∼1−1.15 Mya)	Yuanmou[a], Sangiran, Jianshi (PA1278)[a], Lantian[a]	Grine and Franzen (1994), Kaifu et al. (2005a, b), Wolpoff (1971), Jacob (1973)
Mid-Middle Pleistocene (∼0.7−0.3 Mya)	Zhoukoudian (ZKD), ZKD PA110[a], PA68[a], Xichuan[a], Hexian[a], Yunxian, Yiyuan[a]	Weidenreich (1937)
Late Middle Pleistocene	Jinniushan, Changyang[a], Chaoxian[a], Tongzi[b], Xujiayao[b], Dingcun[b]	He (2000), Bailey and Liu (2010)
Upper Pleistocene (∼110−10 kya)	ZKD Upper Cave, Liujiang[a], Tubo[a], Qingliu[a], Huanglong Cave[a], Longtanshan, Jimuyan	Liu (1999)
Recent Chinese		Brace (1976)
West Asia		
Early Pleistocene	Dmanisi[b]	Martinón-Torres et al. (2008)
Late Middle Pleistocene	Qesem	Hershkovitz et al. (2011)
Upper Pleistocene	Qafzeh, Skhul	Vandermeersch (1981)
Europe		
Early Pleistocene	Atapuerca TD6	Bermúdez de Castro (1993), Bermúdez de Castro et al. (1999)
Middle Pleistocene	Atapuerca SH, Mauer, Arago, Montmaurin, Petralona	Bermúdez de Castro (1986), Howell (1960), Martinón-Torres et al. (2008)
Neanderthals	Arcy II, Chateauneuf, Ehringsdorf, Genay, Spy, Le Moustier, Tabun, Krapina, Lazaret, l'Hortus, La Quina 5, Monsempron, Ochoz, Valdegoba	Leroi-Gourhan (1958), Tillier (1979), de Lumley (1973), Wolpoff (1979), Bermúdez de Castro (1986), Martinón-Torres et al. (2008), Vallois (1952), Vlcek (1969), Quam et al. (2001)
Upper Pleistocene/Holocene recent humans		Brabant (1969)

[a] Observations made on original fossils.
[b] Due to the high degree of occlusal wear, D2600 is not included in the Dmanisi values.

Relative warp analyses (or principal component analysis) of the partial warp scores is conducted to explore the major shape differences through the reduction of the number of variables (Bookstein, 1991; Zelditch et al., 2004).

Landmarks are anatomical loci that are biologically homologous among all specimens (Bookstein, 1991; Zelditch et al., 2004). Four landmarks were selected for each tooth. Landmarks were defined as in Biggerstaff (1969) and Gómez-Robles et al. (2008): the apices

Table 3
Specimens included in the geometric morphometric analysis.

Samples	Specimens	
	P³	P₃
China		
Early Pleistocene	Jianshi (PA1278)[a]	
Mid-Middle Pleistocene (∼0.7−0.3 mya)	ZKD (PA67)[a], Xichuan (PA524)[a], Hexian (PA832)[a], Yiyuan (Sh.y.003)[a], ZKD (Sinanthropus 19)	ZKD (PA110)[a], Xichuan (PA 526)[a], ZKD (Sinanthropus 20, 80, 81, Zdansky)
Late Middle Pleistocene (∼0.3−0.12 mya)	Changyang (PA76)[a], Tongzi (PA873)[a]	
Upper Pleistocene (∼110−10 kya)	Liujiang (PA89)[a], Upper Cave (UP101)	
Indonesia		
Early Pleistocene	Sangiran (S4[a], S7-27[a], S7-31[a], S7-32[a], S7-34[a], S7-58[a])	Sangiran (S6[a], S7-26[a], S7-69[a])
Africa		
Australopithecus	Sterkfontein (Stw 73[a], 183a[a], 192a[a], 252a[a]), Makapansgat (MLD 23[a], MLD 45[a])	Sterkfontein (Stw 14[a], Stw 142[a], Stw 195[a], Stw 233[a], Stw 404[a], Stw 427[a], Stw 498d[a]), Makapansgat (MLD 2[a])
Early Pleistocene	KNM WT-15000[a], KNM ER-3733[a]	KNM WT-15000[a]; KNM ER-992[a] OH 22
West Asia		
Early Pleistocene		Dmanisi (D211, 2375) [a]
Europe		
Early Pleistocene	Atapuerca TD6 (ATD6-7[a], ATD6-69[a])	Atapuerca TD6 (ATD6-3[a])
Middle Pleistocene	Atapuerca SH[a] (AT-41, AT- AT-589, AT-1944, AT-2036, AT-2758, AT-4325, AT-4330, AT-5611, AT-5838, AT-6181) Arago 7	Atapuerca SH[a] (AT-148, AT-563, AT-807, AT-1466, AT-2767, AT- AT-3045, AT-3941, AT-4100, AT-4328), Arago 13
Neanderthals		Krapina (Md-D, E, H), St. Cesaire 1
Upper Pleistocene modern humans		Abri Pataud 1
Recent humans	Chinese (n = 20)[a], South African (n = 20)[a]	Chinese (n = 20)[a], South African (n = 20)[a]

[a] Original fossils included.

of the main buccal and lingual cusps, and the anterior and posterior foveae. However, since wear has flattened the apex of the lingual cusp of the Panxian Dadong P^3, only three landmarks were employed for the geometric morphometric comparison of this tooth.

Semilandmarks are defined as "loci that have no anatomical identifiers but remain corresponding points in a sense satisfactory for subsequent morphometric interpretation" (Bookstein, 1999, p. 177). They can be used to examine the outline shape in lieu of the real landmarks with the combination of sliding techniques, which can minimize the effects of their arbitrary location along the outline (Bookstein, 1991, 1996, 1997; Bookstein et al., 2002; Adams et al., 2004; Gunz et al., 2005). MakeFan6 (Sheets, 2001) was used to define semilandmarks. In MakeFan6, the center of gravity was located in the middle of the crown outline, and from this center thirty fan lines were radiated. The intersection point between a fan line and the crown outline was treated as a semilandmark. For those teeth suffering from significant interproximal wear facets, the original crown outline was estimated by reference to overall shape of the preserved crown and the extent of the wear facets before the localization of semilandmarks (Wood and Uytterschaut, 1987; Gómez-Robles et al., 2008). A series of TPS software (Rohlf, 1998a, b, c) was employed to collect raw coordinate data of the landmarks and semilandmarks and to conduct superimposition and relative warp analyses (or principal component analysis).

Micro-computed tomography and EDJ surface reconstruction

High resolution μCT scanning was performed on the four teeth in order to complement their external morphological description with enamel-dentine junction (EDJ) information. Each tooth was scanned using a 225 kV-μCT scanner equipped with a 1.0-mm aluminum-copper filter under settings of 120 kV, 120 uA, 0.5 angular increment one step, 360 degrees of rotation, 4 frames averaging. Isometric voxel size is 12.70 microns for the P^3 and 16.73 microns for the P₃. Raw projections were converted into image stacks of raw format (tomographic slices) with IVPP225kVC-T_Recon. VGstudio was employed to remove the empty spaces from the image stack to reduce the data size and to save the data as raw volume, which were then imported into Mimics 14.11 to complete the segmentation of enamel and dentine and to visualize the EDJ surfaces.

Description and comparisons of the Panxian Dadong teeth

PDH1 (Panxian Dadong Hominin 1) Right maxillary central incisor (I^1; Figs. 3 and 4)

An adult right I^1 was recovered from sieving of sediments, covered by fallen roof blocks, near the back wall of the cave in 1992. This makes its general provenience approximately 220 m west of the cave entrance and 120 m from the excavation area where the other specimens were found. Although no precise chronological date can be obtained on this tooth, the associated fauna from the brecciated deposit is compatible with a late Middle Pleistocene age estimate of 130–300 ka. The tooth was heavily damaged postmortem, resulting in loss of much of the crown and root. The entire labial enamel surface and some dentine are missing. Except for slight damage to both marginal ridges, the lingual surface of the crown is well preserved with all its morphology intact. The CEJ and a very small portion of the lingual root surface (approximately 2 mm) are also present.

The occlusal wear facet is slightly undulating with dentine exposure along the entire edge. The full extent of the dentine exposure cannot be determined due to breakage, but it is apparent
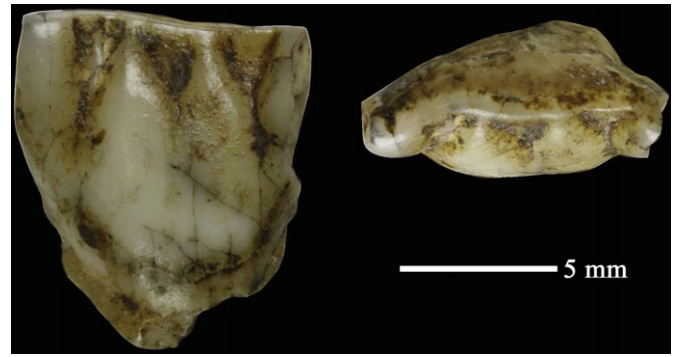

Figure 3. The upper central incisor from Panxian Dadong (left: lingual view, right: occlusal view).

that a substantial portion of the crown height was lost due to attrition. This is apparent from the comparison with more complete incisors (Fig. 9). The wear facet is slightly inclined towards the lingual side, indicating edge-to-edge occlusion during life. According to the Molnar (1971) scoring standard, the wear stage is 5 with extensive dentine exposure. The comparatively higher degree of wear of PDH1 makes it unlikely to be assigned to the same individual as the other Panxian Dadong teeth.

Crown morphology Because of the serious damage to the labial surface, the full crown morphology is no longer visible. However, its relative BL thickness can still be inferred from the remaining dentine, and the crown looks robust. The mesial and distal marginal edges fan out from the crown base towards the incisal edge and from the lingual view the crown has a trapezoid shape. The marginal ridges are well developed and thickened on both the mesial and distal aspects, and this is evident on both the enamel and EDJ surfaces (Fig. 4). These structures make the crown lingual surface prominently shovel-shaped, corresponding with at least ASUDAS grade 5 (Turner et al., 1991). In this context, it is important to note that the ASUDAS was developed to cover the morphological variability of modern populations. The PDH1 morphology, especially the tuberculum dentale conformation, is not fully covered by this classification, so we have also employed Crummett's classification (1995). On the lingual surface, PDH1 expresses a large tuberculum dentale (scored app. grade 5 ASUDAS) that occupies nearly the entire preserved surface of the crown. The tubercle starts at the CEJ in the shape of a swelled eminence and extends towards the incisal edge forming two finger-like extensions of approximately equal size. These two extensions decrease their thickness and end at the current incisal edge, along with a smaller distal extension. The expression of finger-like projections, regardless of the elevation of these from the lingual surface, would fit Crummett's stage 2 of tuberculum dentale expression (Crummett, 1994: 93). These finger-like extensions have their parallel expression on the EDJ surface (Fig. 4). The tubercle morphology and the marginal ridges are delineated by deep grooves that are accentuated by brown staining. From the occlusal view, the substantial loss of crown prevents the assessment of the labial convexity. However, the preserved incisal edge and lingual surface are straight without any curvature. Taking into account our own research (Martinón-Torres, 2006) and Crummett's statement (1995) that the expression of labial convexity corresponds with the expression of lingual concavity, we could suggest from the flatness of the lingual surface and the incisal edge that the labial surface was also probably flat. However, we should be cautious in this statement since this portion of the tooth is not preserved.
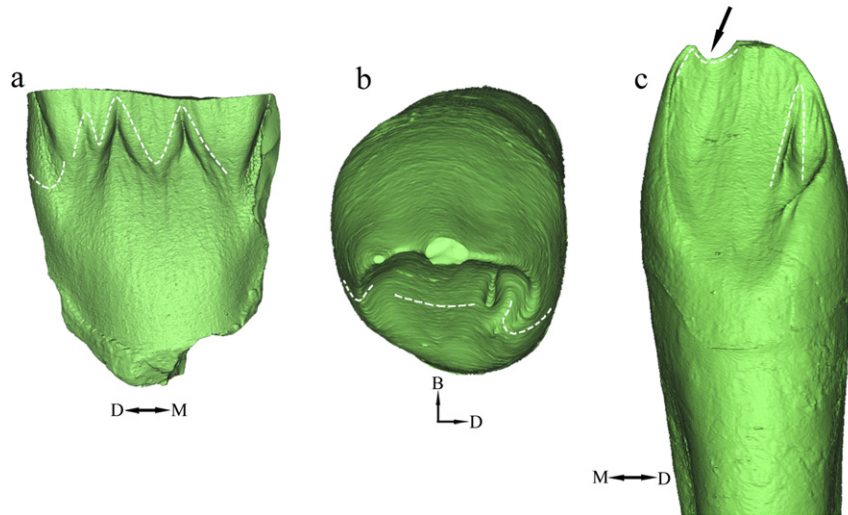
Figure 4. Views of enamel dentine junction (EDJ) of the lingual aspect of the I^1 (a) and the occlusal and lingual aspect of the C_1 (b and c) created from micro-CT scanning. Dotted lines enhance morphological features explained in the text. Arrow points to an indentation in the incisal edge.

Because of the crown damage, only the crown height and MD diameter can be roughly estimated. The crown height was measured as 10.1 mm. If the attritional loss is estimated to be as much as 1/3 of the total crown height, the original height could have been as large as 13 mm. The crown MD dimension was measured as 9.3 mm. If the loss of enamel at the margins is factored in, based on the proportion of crown height and breadth, the actual MD dimension should be around 10.0 mm (Table 3).

PHD2 Right mandibular canine (C_1; Figs. 4 and 5)

An adult right mandibular canine was recovered from sieving the sediment of a test pit, in what is now designated as Area B (square F48) (see Fig. 2), at a depth of 2.28–2.38 m. Based on this general provenience information, the chronological age of this tooth should fall between the lower ESR dates at Dadong (averaging 211 ka (EU) − 257 ka (LU) and correlated with the MIS 8–7
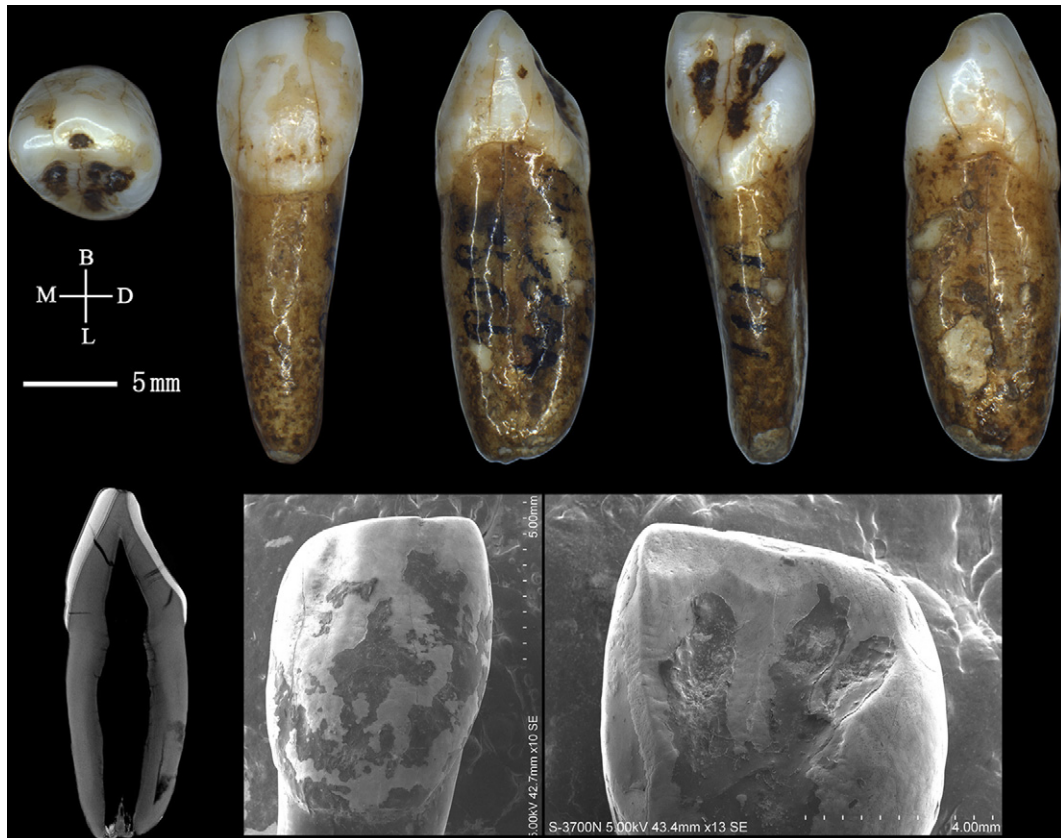

Figure 5. Lower canine from Panxian Dadong. From left to right: occlusal, buccal, mesial, lingual, distal, cross-section from micro-CT scanning and SEM images.

Figure 6. Upper third premolar (P³) from Panxian Dadong (From left to right of the upper row: occlusal, buccal, mesial, lingual, distal; from left to right of the lower row: cross-section from micro-CT scanning, and SEM images of mesial and distal sides.

transition) and the upper ESR dating samples (averaging 137 ka (EU) − 156 ka (LU), and close to MIS 6; Jones et al., 2004; Karkanas et al., 2008).

The tooth is complete with only minor damage to the root tip and thin hairline cracks that invade the enamel on all the tooth surfaces. There is a small semi-circular facet of dentine on the central region of the cutting edge where the cusp has been worn down. The rest of the cutting edge and the upper border of the lingual surface show polished wear facets without dentine exposure. There are also mesial and distal interproximal wear facets. According to Molnar (1971), this tooth presents stage 2 occlusal wear. Differences in size and morphology make it unlikely that this tooth belongs to the same individual as PDH3 or PDH4.

Crown morphology From the labial aspect, the overall crown shape is roughly rectangular with curved lateral sides. The angle between the mesial marginal ridge and the incisal edge is higher and sharper than the distal one but the crown is generally symmetrical.

In lingual view, the central ridge is clear but not particularly full or swollen. It is demarcated by mesial and lingual longitudinal

foveae highlighted by taphonomic brown staining. The faintly elevated lingual central ridge can also be detected on the EDJ surface. Within the distal fovea, a small but well-defined distal accessory ridge (ASUDAS grade 2), can be identified on both the external and EDJ surfaces (Fig. 4). The marginal ridges of the lingual surface are well developed, defining a shovel shape of grade 4 according to the ASUDAS.

Observed from the EDJ surface (Fig. 4), the lingual outline of the crown is elliptical and quite symmetrical. At the mesial portion of the incisal edge, there is a semi-circular notch. The distal marginal ridge is thicker than its mesial counterpart. The mesial and distal marginal ridges merge at the basal region of the crown lingual surface without forming a conspicuous basal eminence, so there is no sign of a tuberculum dentale.

There is also no sign of a buccal cingulum, although the labial/buccal surface is marked by two longitudinal depressions, described as ribbed in the longitudinal direction by Weidenreich (1937; see also SEM image in Fig. 5). These grooves delineate a central and two marginal lobes that merge towards the base of the crown. This appearance is also evident on the EDJ surface in the form of two corresponding longitudinal grooves. From the mesial or distal aspect, the crown is wedge-shaped with a blunted cutting edge. Although there is no cingulum, the basal third of the crown presents a horizontal bulge.

The root of the Panxian Dadong C₁ is stout and straight. It is mesio-distally compressed with the BL dimension greatly exceeding the MD dimension. The maximum BL diameter occurs at approximately the midpoint of the root length and the diameter is then slightly reduced below that point. There are shallow longitudinal furrows on the mesial and distal sides, with the mesial one being deeper and broader.

PDH3 Right upper third premolar (P³; Figs. 6 and 7)

An adult right P³ was discovered during the 1998 excavation at a depth of 1.399 m below the ground surface in square F47 (Fig. 2).
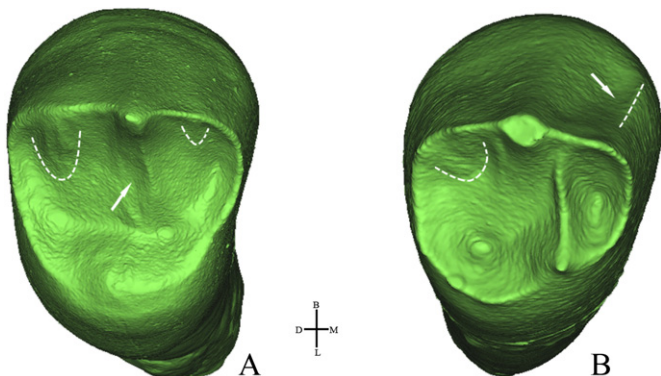

Figure 7. Occlusal views of enamel dentine junction (EDJ) created from micro-CT scanning for the P³ (A) and the P₃ (B).

Figure 8. Lower third premolar (P₃) from Panxian Dadong (From left to right: occlusal, buccal, mesial, lingual, distal and cross-section from micro-CT scanning).

This places it stratigraphically in Layers II–IV with proximity to a tooth sample that yielded an ESR age of 160 ka (EU) – 182 ka (LU) and a Coupled ESR $^{230}Th/^{234}U$ series age of 208 ka+23/−19. These layers are correlated with the glacial interval MIS 6 (Jones et al., 2004; Karkanas et al., 2008).

The tooth has a complete crown and a partial root that is broken at 9.6 mm below the CEJ. The preserved part of the root is in good condition with no visible surface damage, although there are hairline cracks on the mesial and distal sides.

The occlusal wear involves flattening polish on the buccal and lingual cusps. The wear on the lingual cusp is more severe, but there is no dentine exposure. The buccal cusp is less worn, such that the ridges and grooves on the surface are clearly visible. The wear stage corresponds to grade 2 (Molnar, 1971). There is a small interproximal wear facet on the mesial side, but no interproximal wear facet is discernible on the distal side. There is an irregular patch of damaged enamel on the buccal side approximately at the mid-crown level. The enamel border at the central buccal area is not straight, projecting approximately 1.0 mm towards the root and corresponding to grade 1 of enamel extension according to the ASUDAS (Turner et al., 1991). Mesial to this, there is a notable longitudinal depression or groove, running diagonally and upwards from the buccal aspect to the mesial surface, that ends before reaching the mesial longitudinal furrow of the root. SEM images of the groove reveal that the bottom of the groove is smooth and lacks any striations. With the latter observation we discount the explanation that the groove is due to the repeated insertion and retraction of a hard probe or toothpick (Lukacs and Pastor, 1988). We suggest it may be a developmental defect, although further analyses are needed to understand its etiology.

Because of the degree of wear, size and morphology we cannot reject or confirm if this tooth belongs to the same individual as PDH4.

Crown morphology The occlusal surface is composed of the buccal and lingual cusps that are well defined by the sagittal groove. The buccal cusp is clearly larger and wider than the lingual one. The tip of the lingual cusp is mesially displaced in relation to the tip of the buccal one. The sagittal groove extends laterally to end in anterior and posterior foveae that are bordered by mesial and distal marginal ridges. The foveae are shallow and small, with the distal one being slightly deeper than the mesial one. There is no accessory marginal tubercle on the distal or mesial marginal ridges. The essential crest of the buccal cusp is bifurcated by a shallow groove into a larger mesial portion and a distal portion. Although the bifurcation is slight, it is also reflected on the EDJ surface (Fig. 7). Between the essential crest and the mesial marginal ridge there is a short and shallow fissure that delimitates a mesial accessory ridge. This ridge is reflected as a feeble enamel elevation close to the mesial incisal edge on the EDJ surface (see Fig. 7). There is also a distal accessory ridge, which is reflected on the EDJ surface as small dentine elevations. The lingual cusp does not show any relevant features on the outer enamel or EDJ surfaces.

In buccal view, the crown is pentagonal and roughly symmetrical. The mesial occlusal arm is shorter and straighter than the distal one, which has a more pronounced slope. In the latter, we can see the projection of the distal accessory ridge (see below). There are two faint enamel hypoplastic bands (SEM images in Fig. 6) that create a small depression above the crown base. From the mesial and distal views, the base of the crown is swollen, but no cingulum is expressed. Because of the enamel swelling at the crown base, the cervical region looks comparatively constricted. In the mesial and distal views, the buccal cusp is sharper and much higher than the lingual cusp; the latter is blunted by attrition (Fig. 7).

The root is mesiodistally compressed with a slight mesial rotation. Both the mesial and distal sides have broad and shallow grooves starting approximately 2 mm from the CEJ that get deeper

Figure 9. Comparison of the incisor lingual surfaces of Panxian Dadong and other Chinese specimens (From left to right: PDH1, modern human, Huanglong Cave, Dingcun, Tongzi, and Zhoukoudian).

towards the tip and delimit buccal and lingual radicals. However, since the root is broken we cannot ascertain whether or not there was bifurcation.

PDH4 Left lower third premolar (P$_3$; Figs. 7 and 8)

An adult left P$_3$ was discovered during the 2000 excavations at a depth of 1.441 m below the ground surface in square I46 (Fig. 2). Stratigraphically, this places it in Layer VI–VII near a dated sample that yielded an ESR age of 233 ka (EU) − 296 ka (LU) and a Coupled ESR − ^{230}Th/^{234}U age of 294 ka +35/−30. These layers are correlated with the end of glacial MIS 8 and the beginning of interglacial MIS 7 (Jones et al., 2004; Karkanas et al., 2008).

The tooth is well preserved with a complete crown and slight damage to the root tip. There are a few areas of demineralization and concretions on the buccal and lingual aspects of the crown base and upper root, and some hairline cracks.

There is a polished band along the occlusal edge of the buccal cusp with a small island of dentine exposure at the tip. The lingual cusp appears to be unworn. The occlusal wear corresponds to grade 3 of Molnar's (1971) scoring system. There is a small distal interproximal wear facet from contact with the P$_4$, but the mesial interproximal facet from the canine is not discernible.

<u>Crown morphology</u> The shape of the occlusal contour is an asymmetric oval with a disto-lingual bulge due to the development of a distolingual talonid. The maximum occlusal diameter accords with the axis from the mesio-buccal corner to the disto-lingual corner. The buccal cusp is larger than the lingual one and they are connected by a thin but continuous transverse crest that is mesially displaced. This crest is also continuous on the EDJ surface and runs from the mesial aspect of the buccal cusp tip to the middle aspect of the lingual cusp tip (Fig. 7). The tip of the lingual cusp is mesially deviated with regard to the BL axis of the crown and in relation to the tip of the buccal cusp. The posterior fovea is larger and deeper than the anterior one, and this feature is particularly pronounced on the EDJ surface (Fig. 7). There is a small distal accessory ridge between the buccal essential ridge and the distal marginal ridge. This ridge is also reflected in the EDJ as weak enamel elevations (marked with dotted lines in the EDJ in Fig. 7). There is no clear free-tip accessory cusp in the distolingual talonid although there are feeble secondary grooves that stem out of the posterior fovea and seem to delimit up to two accessory ridges or cuspules distal to the metaconid. There is no mesio-lingual groove crossing the marginal ridge. On the EDJ surface the talonid also appears as a distolingual platform without clear free-tip cusps.

In buccal view, the crown shape is essentially pentagonal with the largest MD length at the occlusal edge, exceeding the cervical dimension. Along the cusp edge, the mesial occlusal slope is shorter and straighter than the distal. There are two weak longitudinal furrows delimitating a main central and two marginal ridges on the buccal surface; these are also reflected on the EDJ surface. The expression of the mesial furrow is accentuated by a longitudinal string of pits with brown staining.

In the lingual aspect, there is clear mesial displacement of the metaconid due to the expression of a distolingual talonid. In the mesial or distal views, the difference in height and dimensions between the larger buccal cusp and the lingual one is evident. The buccal surface is inclined and shows some degree of basal bulging, but no cingulum is expressed.

The whole root is slightly divergent towards the distal side, and the root tip is blunt. Both the mesial and distal sides present longitudinal depressions that divide the root into the buccal and lingual radicals, with the lingual one being slightly narrower than the buccal one.

Comparative morphology

I^1

In general, PDH1 presents archaic features, particularly in the degree of expression and complexity of the tuberculum dentale. Finger-like extensions are seen in early *Homo* specimens such as KNM-WT 15000 (M.M-T pers. observation, Martinón-Torres et al., 2008), Zhoukoudian specimens (Weidenreich, 1937), and some Early and Middle Pleistocene hominins such as the Yuanmou incisors, but in these cases they typically show more than two extensions or spines. In contrast, PDH1 is most similar to late Middle Pleistocene hominins from Xujiayao in showing relatively less complex tuberculum dentale conformations and a reduced number of lingual spines. In Middle Pleistocene populations of Europe and Neanderthals, it is more common to find a well-developed and circumscribed basal eminence that can have moderate to pronounced tubercles on its surface, but its expression is usually ridge-shaped (Martinón-Torres et al., 2012). However, a more comprehensive study of the frequency of finger-like extensions in Neanderthals would be desirable to verify this pattern. The tuberculum dentale is also variably expressed in modern humans, depending on the population, but it rarely adopts the shape of finger-like extensions (Weidenreich, 1937; Scott and Turner, 1997).

Shovel shape is another plesiomorphic trait with limited taxonomic discriminative power. It is present in African and Eurasian early *Homo* specimens, but its degree of expression is more pronounced in Asian *Homo erectus*, European Middle Pleistocene groups and, especially, Neanderthals (Mizoguchi, 1985; Crummett, 1994; Bailey, 2000, 2002; Martinón-Torres et al., 2007, 2008, 2012).

Hominin incisors are characterized by a variable degree of labial convexity that is typically more pronounced in Eurasian Pleistocene populations. Unfortunately, the damage on the labial surface of the PD incisor prevents a proper assessment of the labial convexity, but the incisal edge and lingual surface are basically straight. According to Crummett (1995) and our own research (Martinón-Torres, 2006), labial convexity is correlated with lingual concavity, so that the flatness of the lingual surface could be an indirect way of assessing the expression of labial curvature. Greater degrees of labial convexity are typical of, and exclusive to, Eurasian Pleistocene hominins in comparison to their African counterparts (Martinón-Torres et al., 2007). If the flatness of the labial surface of PDH1 could be confirmed, this would be one of the very few derived traits that can be considered typical of *H. sapiens* lineages (Martinón-Torres et al., 2007). However, as the tooth is broken, the assessment has to be taken with caution.

In sum, the Panxian Dadong I^1 exhibits overall archaic features including a well-developed tuberculum dentale with finger-like extensions. The relatively less complex shape of the tuberculum dentale in comparison to the conformations found in Early Pleistocene fossils would be similar to that found in other Chinese late Middle Pleistocene hominins (see Fig. 9).

C$_1$

In general, PDH2 is robust both in the crown and the root aspects. However, its general conformation could be considered derived in comparison to early *Homo* specimens such as *Homo habilis* and the Dmanisi hominins, where the crown is strongly asymmetrical (Tobias, 1991; Martinón-Torres et al., 2008). In later *Homo* specimens, canine shape is more spatulate or incisor-like, although in *Homo ergaster* and some Asian *H. erectus* specimens from Zhoukoudian and Sangiran, the transition between the distal marginal ridge and the distal arm of the incisal edge is low and angled (Weidenreich, 1937; Brown and Walker, 1993; Grine and

Franzen, 1994). In PDH2, the crown is more incisor-like and it does not show any cingulum development, although there is a buccal bulging at the crown base similar to what is found in some Middle Pleistocene fossils of Europe such as Atapuerca − Sima de los Huesos (SH) and Arago (Bermúdez de Castro et al., 2003; Martinón-Torres et al., 2012). This cingulum is also absent in the Sangiran 7 specimens, but it is present in some of the Zhoukoudian specimens. Finally, the median ridge is relatively swollen, similar to the morphology found in *Homo antecessor* (Bermúdez de Castro et al., 1999) and some Middle Pleistocene fossils from North Africa such as Tighennif, Rabat and Sidi-Abderrahaman (and even Jebel Irhoud, despite its later chronology, but not in teeth from Sima de los Huesos). However, the median ridge of the PDH2 does not reach the conspicuous expression that is found in early *Homo* specimens such as the Dmanisi fossils, KNM-ER 992, OH 7 or OH 13, so that a moderate, classic lingual fovea can be identified. Lower canines in modern humans are more slender, and their lingual surface is smoother.

Shovel shape and tuberculum dentale in lower canines are primitive traits with limited diagnostic utility. High frequencies of the strongest degrees of expressions are considered typical of the Neanderthal lineage (Martinón-Torres et al., 2007, 2012) but they are not exclusive to them, being relatively common in early *H. sapiens* and some recent populations (Scott and Turner, 1997; Martinón-Torres et al., 2007). In general, we can state that the Panxian Dadong C_1 retains some primitive features such as a slightly asymmetrical crown shape, a bulging buccal surface, small lingual central ridges, marginal ridges, and robusticity of the root. Yet there is no cingulum, and all of the primitive features are scaled down in their development in comparison with Chinese *H. erectus* in the mid-Middle Pleistocene and the mid- and late Middle Pleistocene specimens from Africa. The Panxian Dadong C_1 is characterized by archaic morphology that is metrically (see below) and morphologically reduced and simplified relative to Early Pleistocene fossils from Africa and Asia and some of the Middle Pleistocene comparative material.

P^3

Compared to Early and Middle Pleistocene hominins from Africa, Asia and Europe, PDH3 shows general derived conformations but these traits are not taxonomically discriminative. The cusps are separated by an uninterrupted central fissure, which is the usual condition in *Homo*, although variable frequencies of the continuous transverse crest are documented in Sangiran *H. erectus* and in the Atapuerca-SH samples (Grine and Franzen, 1994; Martinón-Torres et al., 2012). There is a bifurcated buccal essential crest (or triangular ridge bifurcation, according to Burnett, 1998), a trait that tends to decrease in frequency from the Middle Pleistocene onwards (Martinón-Torres, 2006). Compared to PDH3, Chinese mid-Middle Pleistocene hominins like those from Zhoukoudian are larger and more robust. The whole crown buccal surface of these specimens shows pronounced convexity and usually the mesial and distal ridges are well differentiated from the median ridge (Burnett et al., 2010). It is common to find a buccal cingulum where the mesial portion bulges laterally forming the tuberculum molare. The P^3 from Panxian Dadong presents buccal swelling of the crown, but not a cingulum. Buccal swelling is also common in the Middle Pleistocene fossils from Europe such as Atapuerca-SH, Arago and Neanderthals. However, this swelling is comparatively weaker in PDH3 (see de Lumley et al., 1972; Martinón-Torres et al., 2012). The Panxian Dadong P^3 bears some resemblance to late Middle Pleistocene fossils from China, but these are more primitive. There are two P^3s found in Tongzi, also in the Guizhou Province, which are larger and more

robust, apart from having a cingulum and more complicated occlusal surfaces. One of the Tongzi P^3s (PA521) has three accessory tubercles at each marginal ridge, and the other (PA873) displays up to three well-developed crests on the occlusal aspect of the buccal cusp.

The PDH3 root is robust with two wide radicals, although its appearance is more gracile than the root complex usually found in Zhoukoudian and Chinese Early Pleistocene hominins like Jianshi. In some Sangiran specimens we can see a tendency of further bifurcation of the buccal radical into a distal and a mesial component. European Middle Pleistocene fossils, Neanderthals and *H. sapiens* also share with PDH3 a more gracile root form that is particularly pronounced in recent *H. sapiens* populations. The number of roots is highly polymorphic in *Homo* species so it presents little taxonomic utility. Double rooted upper premolars have been mentioned as characteristic of Neanderthals (de Lumley, 1973) but they can also be found in variable frequencies in European Middle Pleistocene populations and early and recent *H. sapiens* (Scott and Turner, 1997; Martinón-Torres et al., 2012).

The result of the geometric morphometric analysis for P^3s is displayed in Fig. 10. The first two relative warps accounted for 32.9% and 19.89% of the total variance respectively. There is a modern to primitive gradient along RW1. P^3s of recent humans and Chinese Upper Pleistocene hominins are mainly located at the area of the RW1 negative scores. These teeth are characterized by a relatively symmetrical crown outline with a mesiodistally narrower paracone in relation to the protocone. The anterior and posterior foveae are close and the paracone apex is displaced towards the buccal contour. Except for a few examples from the European Middle Pleistocene (Atapuerca-SH) and the Indonesian Early Pleistocene, this area is exclusively occupied by Upper Pleistocene fossils and modern humans. S7-34, S7-58, and PA873 also fall in this area because their protocone is relatively narrow compared to their paracone. On the positive area of RW1 we mostly find *Australopithecus* and Early and Middle Pleistocene specimens from Asia and Europe. P^3s falling in this part of the graph are characterized by a more oval contour where the paracone and protocone are similar in MD width, the paracone apex is more centered in relation to the external outline, and there is a larger distance between the anterior and posterior foveae. The variation along RW2 is less clear, although *Australopithecus* and early Pleistocene fossils from Africa and Europe cluster in the negative score region. They all have oval contours, a larger interfoveal distance and a buccally displaced paracone apex. In the positive area of RW2 we find most of the *H. sapiens* and Middle Pleistocene fossils from Europe, two out of five of the Chinese mid-Middle Pleistocene fossils and half of the Indonesian specimens. Fossils clustering in this region show a relatively narrower lingual half, a shorter interfoveal distance and a paracone apex slightly more centered than those plotting in the negative portion.

The Panxian Dadong P^3 falls in the upper left quadrant, an area that, with the exception of two out of the nine Atapuerca-SH specimens and S7-34, is exclusively occupied by recent humans. Thus this geometric morphometric analysis indicates that the general crown conformation of the Panxian Dadong P^3 resembles some European Middle Pleistocene hominins, Chinese Upper Pleistocene hominins, and particularly the recent human specimens.

According to the above comparisons, the Panxian Dadong P^3 preserves some primitive and highly polymorphic traits, but in general its conformation is derived. Its occlusal morphology is simple, and the contour is symmetrical with a lingual cusp that is narrower than the buccal one. All these features make the Panxian Dadong P^3 most similar to Upper Pleistocene hominins and recent humans in our comparative samples.
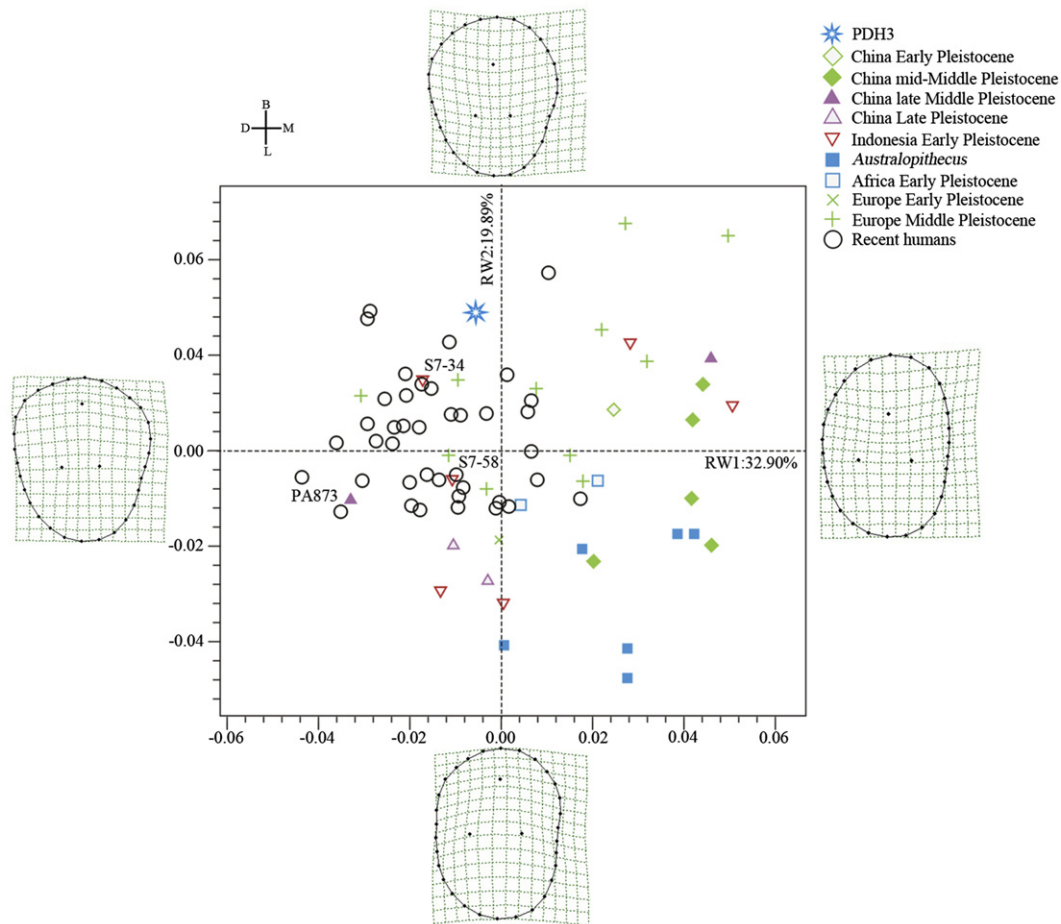
Figure 10. Geometric morphometic analysis of the occlusal shape of the P³ from Panxian Dadong and comparative samples.

P_3

Previous studies (Weidenreich, 1937; Wood and Engleman, 1988; Wood et al., 1988; Tobias, 1991; Bermúdez de Castro et al., 1999; Gómez-Robles et al., 2008; Martinón-Torres et al., 2008; Xing et al., 2009) indicate that the P_3s of African and Asian early hominins (including *Australopithecus*, early *Homo* and *H. erectus*) have a series of typically primitive features such as a pronounced buccal cingulum, a strongly asymmetric occlusal contour with a protruding distolingual talonid, open anterior fovea, robust and complex root systems, and large size. Most of these primitive features can be found in the P_3s of Zhoukoudian and other Chinese mid-Middle Pleistocene hominins.

The P_3 morphology of Upper Pleistocene hominins and recent humans is very different from that of early hominins in many aspects, with nearly all of the primitive features weakly expressed or absent. The occlusal contour of recent human P_3s is basically symmetrical, ranging from completely round contours to those with slight bulging at the distolingual corner (Gómez-Robles et al., 2008; this study). In general, recent humans present simplified occlusal conformations, with weakly developed or absent accessory cusps and ridges, particularly in comparison to earlier hominins (Irish and Guatelli-Steinberg, 2003; Martinón-Torres et al., 2007, 2012). They lack a buccal cingulum and this surfaces tends to be smooth. Roots are generally gracile and awl-shaped, with single roots being the norm although recent populations may show varying degrees of Tomes' root (Scott and Turner, 1997). The

longitudinal furrows along the mesial and distal surfaces of the root are very weak.

European Middle Pleistocene hominins and Neanderthals also have derived conformations with regard to *Australopithecus*, *H. ergaster* and *H. erectus*, but they present a typical conformation characterized by a strongly projected buccal surface on the occlusal plane, a small occlusal polygon (defined by Martinón-Torres et al., 2006 as the occlusal area enclosed by the union of the tips of the main cusps with the anterior and posterior foveae) that is lingually displaced and centrally located with regard to the BL main axis, (Martinón-Torres et al., 2007, 2012; Gómez-Robles et al., 2008), and a bulbous metaconid well-delimited by marginal grooves. These features provide European Middle Pleistocene and Neanderthal P_3s with a canine-like aspect that is not present in Panxian Dadong. PDH4 is less asymmetrical than the P_3s of *Australopithecus*, Early Pleistocene *Homo*, and the Middle Pleistocene specimens found in Africa and Asia, but it is more asymmetrical than the typical P_3 shape found in *H. sapiens* and in the Neanderthal lineage. In addition, PDH4 does not have a mesio-lingual groove, a feature that tends to be common in Neanderthals and *Homo heidelbergensis*.

These morphological differences are also captured by the geometric morphometric analysis in Fig. 11. The PCA graph shows how P_3s of different species plot along RW1 and RW2, which explain 43.97% and 13.29% of the total shape variance respectively. There is a primitive to derived gradient along the first axis. In the negative scores we find premolars with an asymmetrical contour due to distolingual bulging and a wide occlusal polygon due to the buccal

displacement of the protoconid, a comparatively long distance between the anterior and the posterior foveae, and a mesially displaced metaconid with regard to the protoconid. In this part of the graph we find *Australopithecus*, Early Pleistocene *Homo*, and Middle Pleistocene specimens from Africa and Asia. In the region of the positive scores for RW1 we find the majority of the *H. sapiens* specimens, Middle Pleistocene fossils from Europe, and Neanderthals. The variation along RW2 is less clear, with a general overlap of all the groups. With negative scores we find teeth with more asymmetrical contours and a constricted mesiolingual corner, a more centered occlusal polygon, and the axis connecting the anterior and the posterior foveae perpendicular to the main BL axis. In this area we find specimens from all groups. With positive scores we find premolars that are more symmetrical. The metaconid is more mesially displaced and the axis connecting the anterior and the posterior foveae is oblique to the BL axis of the tooth. In this area we find specimens from all groups except West Asian Early Pleistocene fossils and European Upper Pleistocene fossils.

European Middle Pleistocene specimens mainly plot in the positive extreme of the RW1 axis, and three out of the four Neanderthals included in the study overlap with recent humans and European Middle Pleistocene specimens. The other Neanderthal falls in the most negative margin of RW2 because of a strong mesiolingual constriction. The Panxian Dadong P$_3$ plots in the upper left quadrant showing an "attenuated" version of the shapes found in the Asian and European Early Pleistocene specimens, and falling within the range of variation of the recent human specimens from both Asia and Sub-Saharan Africa. It plots close to the quadrant where only *H. sapiens*, one Neanderthal, and some European

Middle Pleistocene fossils cluster. This shows that PDH4 has a slightly asymmetrical crown outline. Moreover, the anterior fovea and the metaconid apex of PDH4 are more buccally positioned. This plot also indicates that the Panxian Dadong P$_3$ is situated among the recent humans with some resemblances to the Chinese mid-Middle Pleistocene and European Middle Pleistocene hominins.

According to the present analysis, the morphological pattern of the Panxian Dadong P$_3$ shows a combination of both primitive and derived features, just like the other teeth from Panxian Dadong. The relatively primitive features include a slightly asymmetrical crown contour, swelling of the crown buccal surface, and a slightly robust root. But in general, all these archaic features are very weakly expressed in the Panxian Dadong P$_3$. For example, the slightly asymmetrical crown contour is caused by the bulging of the disto-lingual portion where no distinct accessory lingual cusps can be ascertained. The transverse crests connecting the two main cusps are thin. The mesial and distal longitudinal furrows on the crown buccal surface are very weak. There is no accessory cusp, tubercle or ridge on the Panxian Dadong P$_3$. There is also no cingulum. The geometric morphometric analysis (Fig. 11) indicates that the crown contour is approximately symmetrical and the polygon is located close to the mesial border with its relative area within the range of recent human variation.

Metric comparison

Table 4 displays the MD and BL dimensions of the Panxian Dadong teeth and those from the comparative sample specified in Table 2. To further compare the metric data, group boxplots for each
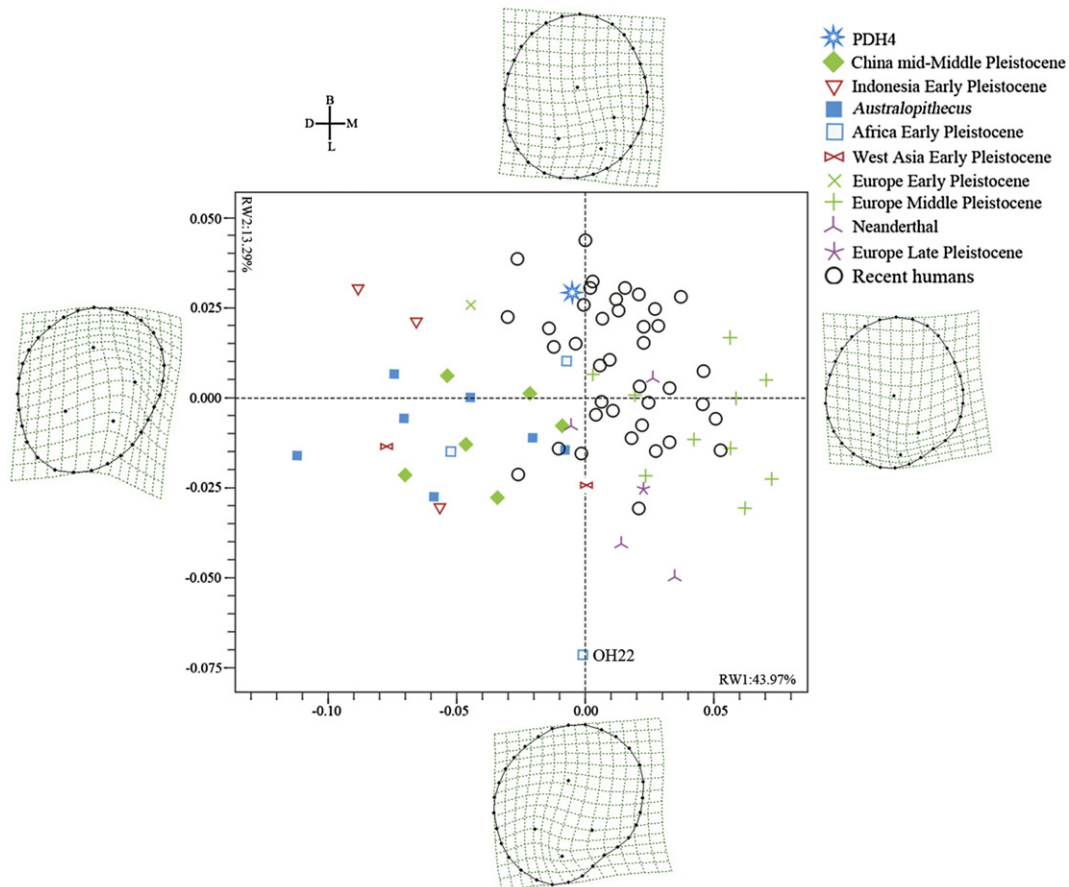

Figure 11. Geometric morphometric analysis of the occlusal shape of the P$_3$ from Panxian Dadong and comparative samples.

Table 4
Tooth metric data for the Panxian Dadong and comparative samples.

Regions	Samples		I^1 MD	C_1 MD	BL	P^3 MD	BL	P_3 MD	BL
Panxian Dadong			(10.0)[a]	7.9	8.3	8.3	10.0	8.2	9.5
East Asia	Early Pleistocene	Mean ± SD	10.5 ± 1.4	8.0	9.2 ± 0.1	8.2 ± 0.7	11.3 ± 1.1	8.1 ± 0.5	9.4 ± 1.3
		Range	8.4–11.5	–	9.1–9.3	7.10–9.5	9.6–12.4	7.7–8.7	8.0–10.6
		N	4	1	3	13	13	3	3
	Mid-Middle Pleistocene	Mean ± SD	10.1 ± 1.3	8.5 ± 0.4	9.1 ± 0.9	8.6 ± 0.6	12.1 ± 0.9	8.5 ± 0.6	9.8 ± 0.7
		Range	7.2–11.7	8.1–9.0	8.2–10.4	7.4–9.2	10.5–12.8	7.9–9.8	8.2–10.8
		N	8	8	8	7	7	17	16
	Late Middle Pleistocene	Mean ± SD	9.5 ± 1.1	–	–	8.5 ± 0.6	11.5 ± 0.9	–	–
		Range	8.3–10.3	–	–	7.4–9.0	10.6–12.8	–	–
		N	3	–	–	5	5	–	–
	Upper Pleistocene	Mean ± SD	8.4 ± 0.3	7.3 ± 0.5	8.8 ± 0.4	7.3 ± 0.8	10.2 ± 0.3	7.4 ± 1.0	8.2 ± 0.8
		Range	8.0–9.0	6.4–7.8	8.3–9.2	6.2–8.0	9.8–10.7	6.9–8.8	7.1–8.9
		N	9	6	7	6	6	4	4
	Recent H. sapiens	Mean ± SD	8.3 ± 0.4	6.8 ± 0.4	7.8 ± 0.6	7.1 ± 0.4	9.4 ± 0.5	6.8 ± 0.7	8.2 ± 0.6
		N	35	41	41	40	40	36	36
West Asia	Early Pleistocene	Mean ± SD	12.6	9.3 ± 0.8	8.9 ± 0.6	8.6	11.6	9.2 ± 0.4	10.1 ± 0.2
		Range		8.4–9.8	7.8–9.5		–	–	8.8–9.7
		N	1	3	3	1	1	4	4
	Late Middle Pleistocene	Mean ± SD	9.53	7.2	8.3	8.5	11.5	7.3	7.6
		Range	–	–	–		–	–	–
		N	3	1	1	1	1	1	1
	Upper Pleistocene	Mean ± SD	9.9	8.2 ± 0.7	9.1 ± 0.9	7.6 ± 0.5	10.4 ± 0.5	8.0 ± 0.5	9.0 ± 0.5
		Range	9–11.1	7.5–8.8	7.8–9.9		7.0–8.3	10.0–11.1	7.5–8.5
		N	6	4	4	8	7	5	4
Africa	Early Pleistocene	Mean ± SD	11.5	8.9 ± 0.5	8.8 ± 0.9	9.0 ± 0.8	12.3 ± 0.9	9.5 ± 0.6	10.4 ± 1.0
		Range	10.2–12	5.4–7.8	7.1–9.6		7.7–10.2	11.0–13.8	8.6–10.4
		N	4	6	6	12	12	10	10
	Middle Pleistocene North Africa	Mean ± SD	–	8.3	8.8	8.5	12.0	9.0 ± 0.8	10.2 ± 0.6
		Range		–	–		–	8.4–10.3	9.6–11.2
		N	–	3	4	1	1	5	5
Europe	Early Pleistocene	Mean ± SD	–	8.1	10	8.6 ± 0.3	11.6 ± 0.2	8.4	10.2
		Range		–	–	8.4–8.8	11.5–11.7	8.0–8.8	9.9–10.6
		N	–	1	1	3	3	2	2
	Middle Pleistocene	Mean ± SD	9.6	7.6 ± 0.4	8.7 ± 0.7	7.9 ± 0.5	10.5 ± 0.7	8.0 ± 0.4	9.0 ± 0.7
		Range	8.7–10.8	6.9–8.5	7.3–10.1		7.10–9.1	9.2–12.0	7.0–9.0
		N	29	32	32	31	32	37	36
	Neanderthals	Mean ± SD	10.2	7.9 ± 0.5	9.1 ± 0.7	7.9 ± 0.7	10.7 ± 0.6	7.9 ± 0.6	9.0 ± 0.8
		Range	9.4–11.1	6.4–8.8	7.5–10.3		6.5–9.3	9.0–11.9	5.8–9.2
		N	18	30	30	38	37	47	46
	Upper Pleistocene/recent humans	Mean	8.6	7.3	8.4	6.9	9.4	7	8.2
		N	19	28	26	21	21	29	29

[a] Value in brackets is an estimation.

diameter are given in Figs. 12–15. Although the comparison of isolated tooth dimensions provides very limited reliable taxonomic information, it is possible to obtain general assessments about metric trends (e.g., Wolpoff, 1971; Bermúdez de Castro and Nicolás, 1995).

As shown in Table 4 and the boxplots in Fig. 12, the estimated MD dimension of the Panxian Dadong I^1 (PDH1) overlaps with the measurements of all the groups except the Upper Pleistocene of East Asia, and the Early Pleistocene hominins from West Asia and Africa. The MD breadth of PDH1 is close to the mean of other late Middle Pleistocene hominins from East and West Asia, the European Middle Pleistocene specimens, and also Neanderthals.

The MD dimension of the Panxian Dadong lower canine (PDH2) is outside the range of variation of Early Pleistocene canines from Asia and Europe as well as the mid-Middle Pleistocene teeth from East Asia (Fig. 13). It overlaps with the Middle and Upper Pleistocene groups of West Asia, Africa and Europe, and the Neanderthals. Unfortunately, we lack any lower canines from the late Middle Pleistocene in East Asia for comparison, but the Panxian Dadong tooth is smaller than the African late Middle Pleistocene specimen from Jebel Irhoud.

The BL dimension of the Panxian Dadong canine is generally small, and falls outside of the range of variation for Early Pleistocene hominins from East Asia and Europe and the Upper Pleistocene specimens of East Asia (Fig. 13). It is close to the mean of late Middle and Upper Pleistocene hominins and recent humans.

The P^3 MD dimensions show a general overlap among groups. Early Pleistocene teeth tend to have larger dimensions and, in general terms, the PDH3 MD size falls within the ranges of variation of Middle and Upper Pleistocene hominins, with the exception of the Upper Pleistocene groups from East Asia (Table 4; Fig. 14). Regarding the BL diameter, nearly all the samples used in the present study have larger BL diameters than PDH3, which is outside of the ranges of variation of the African and Asian Middle Pleistocene groups, and similar to Upper Pleistocene values from Asia.

As shown in Table 4 and Fig. 15, the MD crown dimension of the Panxian Dadong P_3 (PDH4) is smaller and outside the range of variation of Early Pleistocene teeth from West Asia and Africa. Compared with the Middle Pleistocene hominins, the MD length of PDH4 is smaller than African Middle Pleistocene hominins, but is close to, or larger than the means of the Asian and European groups,
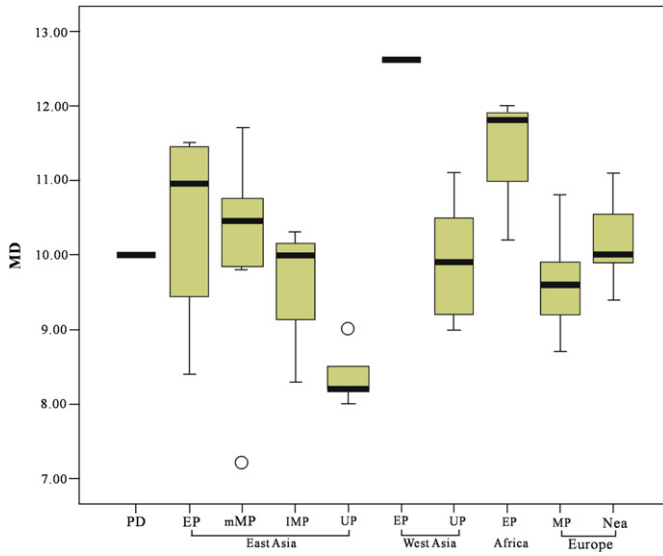
Figure 12. Boxplots of I^1 MD dimensions for Panxian Dadong and comparative samples. (EP = Early Pleistocene; MP = Middle Pleistocene; UP = Upper Pleistocene; Nea = Neanderthals; mMP = mid-Middle Pleistocene; lMP = late Middle Pleistocene).

including the Neanderthals. The P$_3$ BL dimension is smaller and outside the ranges of variation of the Early Pleistocene hominins from West Asia and Europe, and the Middle Pleistocene fossils from Africa. But it is also larger and outside of the ranges of variation of Upper Pleistocene groups from East Asia and the late Middle Pleistocene fossil from West Asia.

These metric comparisons indicate that the PD I^1 and P$_3$ are relatively large, and within the ranges of Middle Pleistocene populations. However, the MD and BL dimensions of the C$_1$ and P^3 are smaller, and closest to those of Eurasian late Middle Pleistocene samples and early *H. sapiens*.

Discussion and conclusions

Although there have been some late Middle and Upper Pleistocene hominin fossils found in China, the morphological

information about these populations is still limited and not well-known by the general paleoanthropological community. There are controversies and inconclusive discussions concerning their morphology, taxonomy, and phylogenetic relationships with later hominin lineages (e.g., Bräuer, 1984; Wu and Poirier, 1995; Etler, 1996; Shang et al., 2007; Liu et al., 2010a, b). This lack of consensus, and the frequent publication of these materials in non-English scientific journals, has had an impact on the recognition of the importance of these specimens for investigating the evolutionary trends of Middle Pleistocene hominins and the origins of the *H. sapiens* lineage.

Several Middle and Upper Pleistocene sites in southern China and the regions bordering the Yangtze River have provided hominin fossils pertinent to this discussion (Wu and Poirier, 1995; Liu et al., 2010a, b). Some of them, including Chaoxian, Tongzi, Maba and Changyang, are contemporary with Panxian Dadong. The morphological and metric comparisons of the Panxian Dadong teeth in the present study are not conclusive in terms of their taxonomic placement. However, it is possible to outline some morphological and metric derived traits that align these teeth with other late Middle and Upper Pleistocene fossils of Asia, and in general indicate the Panxian Dadong teeth are more derived than teeth from other Chinese late Middle Pleistocene localities. Of course, we cannot forget that we have only four isolated teeth and the size of this sample necessarily limits the extent of our conclusions. In addition, most of these derived traits are not diagnostic in terms of linking Panxian Dadong to any particular known lineage, including anatomically modern *H. sapiens*. However, the relatively derived nature of these teeth gives us pause for thought about the origin of *H. sapiens* in this region.

The Panxian Dadong I^1 and C$_1$ present more archaic features than the P$_3$ and the P^3. The I^1 is robust with a marked tuberculum dentale with finger-like extensions, although that feature is comparatively less complex than the morphologies of the Chinese mid-Middle Pleistocene fossils of *H. erectus*. The lower canine is robust but symmetrical in crown shape and it lacks any trace of a cingulum. The Panxian Dadong P^3 displays more derived traits, falling within the range of variation of some European Middle Pleistocene hominins, Chinese Upper Pleistocene hominins, and particularly, West Asian early modern humans. Finally, the Panxian Dadong P$_3$ combines some archaic and derived features that are commonly
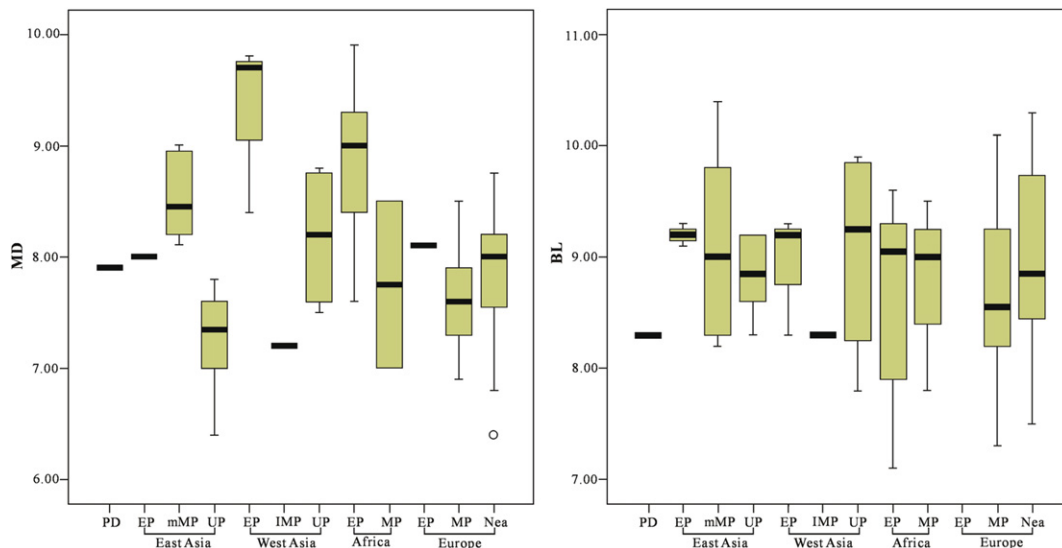

Figure 13. Boxplots of mandibular canine MD and BL dimensions for Panxian Dadong and comparative samples. (EP = Early Pleistocene; MP = Middle Pleistocene; UP = Upper Pleistocene; Nea = Neanderthals; mMP = mid-Middle Pleistocene; lMP = late Middle Pleistocene).
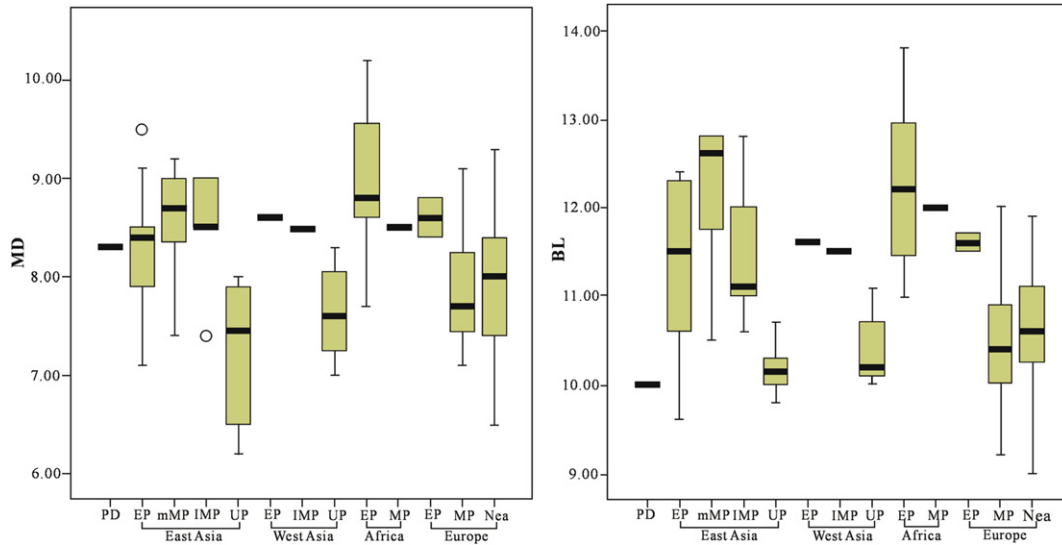
Figure 14. Boxplots of P³ MD and BL dimensions for Panxian Dadong and comparative samples. (EP = Early Pleistocene; MP = Middle Pleistocene; UP = Upper Pleistocene; Nea = Neanderthals; mMP = mid-Middle Pleistocene; lMP = late Middle Pleistocene).

found in Chinese mid-Middle Pleistocene hominins, European Middle Pleistocene populations, and recent humans. This mosaic of primitive and derived traits gives a glimpse of the high morphological diversity of the prehistoric populations that inhabited the vast geographical region of East Asia and raises the possibility of new evolutionary trends that have yet to be fully understood. Upper Pleistocene fossils from Africa and Europe have been generally classified as *H. sapiens* or *Homo neanderthalensis*. However, comparatively little is known about the evolution of human populations in Asia and the question remains how to relate late Middle Pleistocene and Upper Pleistocene fossils from Asia to either *H. sapiens*, Neanderthals, or to something else unique to Asia. Although the Panxian Dadong teeth overlap in some morphological trends and in their dimensions with European Middle Pleistocene groups and the Neanderthals, they do not show any of the so-called typical Neanderthal traits nor any apomorphic feature that allow us to directly relate them to *H. sapiens*. However, our analysis reveals that the Panxian Dadong fossils are generally more derived than the

Pleistocene fossils from North Africa, including the roughly contemporaneous C_1 from Jebel Irhoud.

The limitations for defining the phylogenetic position of Panxian Dadong with regard to later hominin lineages derives from the relative scarcity of fossil remains and the lack of apomorphic features to specifically link these remains to Neanderthals or *H. sapiens* groups. This problem is not exclusive to the Panxian Dadong sample, as it is common to the Middle Pleistocene records of Africa and Asia. By contrast, for the European Middle Pleistocene hominins, and despite the controversies about their taxonomic assignment, there is a general consensus about the phylogenetic link of these populations with Neanderthals (e.g., Stringer, 1985; Rightmire, 2008; Hublin, 2009; Tattersall and Schwartz, 2009; Dennell et al., 2011; Martinón-Torres et al., 2011, 2012). The phylogenetic position of the Middle Pleistocene fossils of Africa is less clear, and this is partially due to the scarcity of the fossil record for this period and region. On dental grounds, the African Middle Pleistocene record consists of some mandibles and associated teeth recovered from
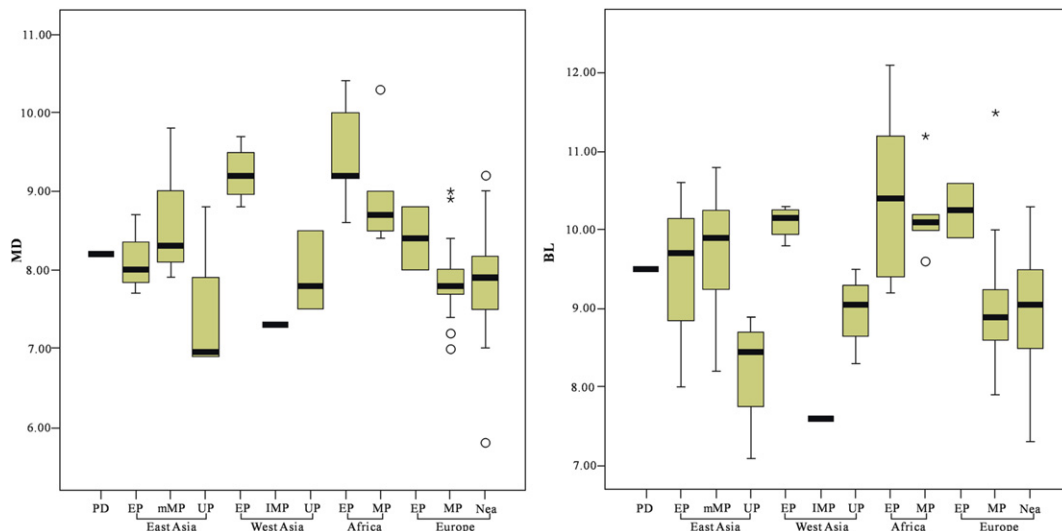

Figure 15. Boxplots of P₃ MD and BL dimensions for Panxian Dadong and comparative samples. (EP = Early Pleistocene; MP = Middle Pleistocene; UP = Upper Pleistocene; Nea = Neanderthals; mMP = mid-Middle Pleistocene; lMP = late Middle Pleistocene).

sites such as Tighennif, Rabat, Thomas' Quarrry, and Jebel Irhoud. The taxonomic and phylogenetic affiliation of these fossils is still a matter of debate. According to some authors, the North Africa Middle Pleistocene record represents the ancestry of *H. sapiens* (Hublin and Tillier, 1981; Hublin and Tillier, 1981, 2001). However, a detailed phenetic and cladistic analysis of the Tighennif dentognathic sample has not revealed any apomorphic traits that can specifically link these fossils to the *H. sapiens* lineage. Tighennif could therefore represent portions of an isolated African Early Pleistocene lineage (Martinón-Torres et al., 2007; Bermúdez de Castro et al., 2008). Similarly, the Jebel Irhoud lower canine, approximately contemporaneous with Panxian Dadong, shows noticeably more primitive traits than Panxian Dadong, including a remarkable size, an asymmetric labial/lingual contour and a conspicuous median ridge. These differences between the African and Asian Middle Pleistocene human assemblages may be pointing to different evolutionary trends for the populations of both continents and raise a number of unsolved questions about the evolutionary story of humans during the Middle Pleistocene. Current data and research have not yet confirmed or disproved whether late Middle Pleistocene and Upper Pleistocene hominins from Asia can fit within the variability of *H. sapiens* or Neanderthals, whether they are the result of the evolution in isolation of *H. erectus*, or whether they may even represent a fourth hominin lineage distinctive to Asia.

We believe that the key to understanding the evolutionary fate of the Middle Pleistocene populations from Africa and Asia will derive from future fossil discoveries and more precise chronologies that help build a comparable fossil record and chronological framework between the continents. In the meantime, it is necessary to further investigate the polarity of morphological features present in the Middle Pleistocene groups and to identify Neanderthal and/or *H. sapiens* apomorphic traits. The identification of apomorphic dental features for *H. sapiens* might thus be a crucial issue in tracing the time and location of its origin from a paleontological point of view. Only a few traits have been suggested as autapomorphic for this lineage, such as completely flat labial surfaces or the total absence of shovel shape in incisors (Martinón-Torres et al., 2007). However, those traits are polymorphic and not necessarily representative of all *H. sapiens* specimens. As discussed above, if the flatness of the labial surface of PDH1 could be confirmed, this would be an important feature suggesting an evolutionary trend towards *H. sapiens* (Martinón-Torres et al., 2007). As an example of the problems derived from the contested polarity of these features, the new Middle Pleistocene dental remains from the Qesem Cave (Israel) have been published as displaying similarities with the Skhul and Qafzeh material but also with Neanderthals (Hershkovitz et al., 2011). Along the same lines, recent studies suggest that some derived "Neanderthal" features are not "Neanderthal" apomorphies but traits that appeared in an ancestral and polymorphic population in the Early Pleistocene (Martinón-Torres et al., 2006, 2007; Bermúdez de Castro et al., 2012). This situation could potentially explain the preservation of "Neanderthal" features in early *H. sapiens* groups (Martinón-Torres et al., 2012) and *less defined* morphologies in the populations close to the node of divergence.

The aim of this paper was to present the late Middle Pleistocene hominin teeth from Panxian Dadong in South China, and to contribute new data for the discussion of evolutionary trends in the Middle Pleistocene populations of Asia. The understanding of the phylogenetic position of these groups represents a crucial step toward further exploration of the origin of later hominin lineages. Fossil discoveries and research of the last decade suggest that the appearance of modern humans in Asia may be earlier than was previously thought (Liu et al., 2010a, b; Hershkovitz et al., 2011);

these results and the present study highlight the necessity of incorporating this new Asian evidence into the scientific debate about human evolution and the development of dental diversity in *Homo* lineages.

Acknowledgments

References

Adams, D.C., Rohlf, F.J., Slice, D.E., 2004. Geometric morphometrics: ten years of progress following the 'Revolution'. Ital. J. Zool. 71, 5–16.

Bailey, S.E., 2000. Dental morphological affinities among Late Pleistocene and recent humans. Dental Anthropol. 14, 1–8.

Bailey, S.E., 2002. Neandertal dental morphology: implications for modern human origins. Ph.D. dissertation, Arizona State University.

Bailey, S., Liu, W., 2010. A comparative dental metrical and morphological analysis of a Middle Pleistocene hominid maxilla from Chaoxian (Chaohu). Quatern. Int. 211, 14–23.

Bermúdez de Castro, J.M., 1986. Dental remains from Atpauerca (Spain) I. Metrics. J. Hum. Evol. 15, 265–287.

Bermúdez de Castro, J.M., 1988. Dental remains from Atapuerca/Ibeas (Spain) II. Morphology. J. Hum. Evol. 17, 279–304.

Bermúdez de Castro, J.M., 1993. The Atapuerca dental remains: new evidence (1987–1991 excavations) and interpretations. J. Hum. Evol. 24, 339–371.

Bermúdez de Castro, J.M., Carretero, J.M., García-González, R., Rodríguez-García, L., Martinón-Torrres, M., Rosell, J., Blasco, R., Martín-Francés, L., Modesto, M., Carbonell, E., 2012. Early Pleistocene human humeri from the Gran Dolina-TD6 site (Sierra de Atapuerca, Spain). Am. J. Phys. Anthropol. 147, 604–607.

Bermúdez de Castro, J.M., Martinón-Torres, M., Carbonell, E., Sarmiento, S., Rosas, A., Van der Made, J., Lozano, M., 2004. The Atapuerca sites and their contribution to the knowledge of human evolution in Europe. Evol. Anthropol. 13, 25–41.

Bermúdez de Castro, J.M., Martinón-Torres, M., Gómez-Robles, A., Prado, L., Sarmiento, S., 2008. Comparative analysis of the Gran Dolina-TD6 (Spain) and Tighennif (Algerie) hominin mandibles. Bull. Mém. Soc. Anthropol. Paris 19, 149–167.

Bermúdez de Castro, J.M., Martinón-Torres, M., Sarmiento, S., Lozano, M., 2003. Gran Dolina-TD6 versus Sima de los Huesos dental samples from Atapuerca: evidence of discontinuity in the European Pleistocene population? J. Archaeol. Sci. 30, 1421–1428.

Bermúdez de Castro, J.M., Nicolás, M.E., 1995. Posterior dental size reduction in hominids: the Atapuerca evidence. Am. J. Phys. Anthropol. 96, 335–356.

Bermúdez de Castro, J.M., Rosas, A., Nicolás, M.E., 1999. Dental remains from Atapuerca-TD6 (Gran Dolina site, Burgos, Spain). J. Hum. Evol. 37, 523–566.

Biggerstaff, R.H., 1969. The basal area of posterior tooth crown components: the assessment of within tooth variation of premolars and molars. Am. J. Phys. Anthropol. 31, 163–170.

Bookstein, F.L., 1989. Principal warps: thin-plate splines and the decomposition of deformations. IEEE Trans. Pattern Anal. Mach. Intell. 11, 567–585.

Bookstein, F.L., 1991. Morphometric Tools for Landmark Data. Cambridge University Press, Cambridge.

Bookstein, F., 1996. Applying landmark methods to biological outline data. In: Mardia, K.V., Gill, C.A., Dryden, I.L. (Eds.), Image Fusion and Shape Variability Techniques. Leeds University Press, Leeds.

Bookstein, F.L., 1997. Landmark methods for forms without landmarks: morphometrics of group differences in outline shape. Med. Image Anal. 1, 225–243.

Bookstein, F.L., 1999. Linear methods for nonlinear maps: procrustes fits, thin plate splines, and the biometric analysis of shape variability. In: Toga, A. (Ed.), Brain Warping. Academic Press, San Diego, pp. 157–181.

Bookstein, F.L., Sampson, P.D., Connor, P.D., Streissguth, A.P., 2002. Midline corpus callosum is a neuroanatomical focus of fetal alcohol damage. Anat. Rec. New Anat. 269, 162—174.

Brabant, H., 1969. La denture humaine au Paléolithique supérieur d' Europe. In: Camps, G., Olivier, G. (Eds.), L'Homme de Cro-Magnon. Arts et Métiers Graphiques, Paris, pp. 99—119.

Brace, L., 1976. Tooth reduction in the orient. Asian Perspective 19, 203—219.

Brace, L., 1984. Prehistoric and modern tooth size in China. In: Smith, F.H., Spencer, F. (Eds.), The Origin of Modern Humans. Alan R Liss Inc, New York, pp. 485—516.

Bräuer, G., 1984. The "Afro-European *sapiens* hypothesis", and hominid evolution in East Asia during the late Middle and Upper Pleistocene. Cour. Forsch. Inst. Senckenberg 69, 145—165.

Brown, B., Walker, A., 1993. The dentition. In: Walker, A., Leakey, R. (Eds.), The Nariokotome Homo Erectus Skeleton. Springer-Verlag, Berlin, pp. 161—192.

Burnett, S.E., 1998. Maxillary premolar accessory ridges: worldwide occurrence and utility in population differentiation. M.A. thesis, Arizona State University.

Burnett, S.E., Hawkey, D.E., Turner II, C.G.1, 2010. Population variation in human maxillary premolar accessory ridges (MxPAR). Am. J. Phys. Anthropol. 141, 319—324.

Crummett, T., 1994. The evolution of shovel shaping: regional and temporal variation in human incisor morphology. Ph.D. dissertation, University of Michigan.

Crummett, T., 1995. The three dimensions of shovel-shaping. In: Moggi-Cecchi, F. (Ed.), Aspects of Dental Biology: Palaeontology, Anthropology and Evolution. International Institute for the Study of Man, Florence, pp. 305—313.

Dennell, R.W., Martinón-Torres, M., Bermúdez de Castro, J.M., 2011. Hominin variability, climatic instability and population demography in Middle Pleistocene Europe. Quat. Sci. Rev. 30, 1151—1524.

de Lumley, H., de Lumley, M.-A., Brandi, R., Guerrier, E., Pillard, F., Pillard, B., 1972. La Grotte Mouste' rienne de Hortus. Editions du Laboratoire de Paléontologie Humaine et de Préhistoire, Marseille.

de Lumley, M.A., 1973. Anténéandertaliens et Néandertaliens du Bassin Méditerranéen Occidental Européen. In: Études quaternaires, mém, vol. 2. Université de Provence, Marseille.

Diedrich, C., 2010. Specialized horse killers in Europe: foetal horse remains in the Late Pleistocene Srbsko Chlum-Komín Cave hyena den in the Bohemian Karst (Czech Republic) and actualistic comparisons to modern African spotted hyenas as zebra hunters. Quatern. Int. 220, 174—187.

Ennouchi, E., 1976. Un deuxième Archanthropien à la carrière Thomas III (Maroc). Bull. Mus. Natn. Hist. Nat. 397, 273—296.

Etler, D., 1996. The fossil evidence for human evolution in Asia. Annu. Rev. Anthropol. 25, 275—301.

Gómez-Robles, A., Martinón-Torres, M., Bermúdez de Castro, J.M., Margvelashvili, A., Bastir, M., Arsuaga, J.L., Pérez-Pérez, A., Estebaranz, F., Martínez, L.M., 2007. A geometric morphometric analysis of hominin upper first molar shape. J. Hum. Evol. 53, 272—285.

Gómez-Robles, A., Martinón-Torres, M., Bermúdez de Castro, J.M., Prado, L., Sarmiento, S., Arsuaga, J.L., 2008. Geometric morphometric analysis of the crown morphology of the lower first premolar of hominins, with special attention to Pleistocene *Homo*. J. Hum. Evol. 55, 627—638.

Gómez-Robles, A., Martinón-Torres, M., Bermúdez de Castro, J.M., Prado-Simón, L., Arsuaga, J.L., 2011. A geometric morphometric analysis of hominin upper premolars. Shape variation and morphological integration. J. Hum. Evol. 61, 688—702.

Grine, F.E., Franzen, J.L., 1994. Fossil hominid teeth from the Sangiran Dome (Java, Indonesia). Cour. Forsch.-Inst. Senckenberg 171, 75—103.

Gunz, P., Mitteroecker, P., Bookstein, F.L., 2005. Semilandmarks in three dimensions. In: Slice, D. (Ed.), Modern Morphometrics in Physical Anthropology. Kluwer Academic/Plenum Publishers, New York, pp. 73—98.

He, J., 2000. Preliminary study of the teeth of Jinniushan archaic *Homo sapiens*. Acta Anthropol. Sinica 19, 217—225.

Hershkovitz, I., Smith, P., Sarig, R., Rolf, Q., Rodríguez, L., García, R., Arsuaga, J., Barkai, R., Gopher, A., 2011. Middle Pleistocene dental remains from Qesem Cave (Israel). Am. J. Phys. Anthropol. 144, 575—592.

Howell, F.C., 1960. European and Northwest African middle Pleistocene hominids. Curr. Anthropol. 1, 195—232.

Huang, W., (Ed.), 1997. Special issue of the studies of the paleolithic site of Panxian Dadong, Guizhou (1991—1993). Acta Anthropol. Sinica 16, 171—254.

Huang, W., Hou, Y., 1997. Stone industry from Panxian Dadong, a cave-site of southeastern China. Acta Anthropol. Sinica 16, 171—189.

Huang, W., Si, X., Hou, Y., Miller-Antonio, S., Schepartz, L.A., 1995. Excavations at the stratified Cave of Panxian Dadong, Guizhou Province, Southern China. Curr. Anthropol. 36, 844—846.

Hublin, J.-J., 2001. Northwestern African Middle Pleistocene hominids and their bearing on the emergence of *Homo sapiens*. In: Barham, L., Robson-Brown, K. (Eds.), Human Roots: Africa and Asia in the Middle Pleistocene. Western Academic and Specialist Press, Bristol, pp. 99—121.

Hublin, J.-J., 2009. The origin of Neanderthals. Proc. Natl. Acad. Sci. USA 106, 16022—16027.

Hublin, J.J., Tillier, A.M., 1981. The Mousterian juvenile mandible from Irhoud (Morocco): a phylogenetic interpretation. In: Stringer, C.B. (Ed.), Aspects of Human Evolution. Taylor & Francis, London, pp. 167—185.

Irish, J.D., Guatelli-Steinberg, D., 2003. Ancient teeth and modern human origins: an expanded comparison of African Plio-Pleistocene and recent world dental samples. J. Hum. Evol. 45, 113—144.

Jacob, T., 1973. Paleoanthropological discoveries in Indonesia with special reference to the finds of the last two decades. J. Hum. Evol. 2, 473—485.

Jones, H.L., Rink, W.J., Schepartz, L.A., Miller-Antonio, S., Huang, W., Hou, Y., Wang, W., 2004. Coupled electron spin resonance (ESR)/Uranium-series dating of mammalian tooth enamel at Panxian Dadong, Guizhou Province, China. J. Arch. Sci. 31, 965—977.

Kaifu, Y., Aziz, F., Baba, H., 2005a. Hominid mandibular remains from Sangiran: 1952—1986 collection. Am. J. Phys. Anthropol. 128, 497—519.

Kaifu, Y., Baba, H., Aziz, F., Indriati, E., Schrenk, F., Jacob, T., 2005b. Taxonomic affinities and evolutionary history of the early Pleistocene hominids of Java: dentognathic evidence. Am. J. Phys. Anthropol. 128, 709—726.

Karkanas, P., Schepartz, L., Miller-Antonio, S., Wang, W., Huang, Wei, 2008. Pleistocene climate in southwestern China: inferences from the Stratigraphic record of Panxian Dadong Cave, Guizhou. Quatern. Sci. Rev. 27, 1555—1570.

Kimbel, W.H., Rak, Y., Johanson, D.C., 2004. The Skull of *Australopithecus afarensis*. Oxford University Press, New York.

Lefêvre, J., 1973. Etude odontologique des homes de Muge. Bull. Mém. Soc. Anthropol. Paris 12, 301—333.

Leroi-Gourhan, A., 1958. Etude des restes humaines fossiles provenant des grottes d'Arcy-Sur-Cure. Ann. Paléontol. 44, 87—148.

Liu, W., 1999. The evolution of tooth size of Quaternary humans in China. Quatern. Res. 2, 127—138.

Liu, W., Jin, C., Zhang, Y., Cai, Y., Xing, S., Wu, X., Cheng, H., Edwards, L., Pan, W., Qin, D., An, Z., Trinkaus, E., Wu, X., 2010a. Human remains from Zhirendong, South China, and modern human emergence in East Asia. Proc. Natl. Acad. Sci. USA 107, 19201—19206.

Liu, W., Wu, X.,Z., Pei, S., Wu, X.J., 2010b. A preliminary report on Huanglong Cave: a Late Pleistocene human fossil site in Hubei Province, China. Quatern. Int. 211, 29—41.

Liu, W., Si, X., 1997. The human teeth discovered in Dadong, Panxian County, Guizhou Province. Acta Anthropol. Sinica 16, 193—200.

Lukacs, J.R., Pastor, R.F., 1988. Activity-induced patterns of dental abrasion in prehistoric Pakistan: evidence from Mehrgarh and Harappa. Am. J. Phys. Anthropol. 76, 377—398.

Martinón-Torres, M., 2006. Evolución del aparato dental en homínidos: estudio de los dientes humanos del Pleistoceno de la Sierra de Atapuerca (Burgos). Ph.D. Dissertation, Universidad de Santiago de Compostela.

Martinón-Torres, M., Bastir, M., Bermúdez de Castro, J.M., Gómez, A., Sarmiento, S., Muela, A., Arsuaga, J.L., 2006. Hominin lower second premolar morphology: evolutionary inferences through geometric morphometric analysis. J. Hum. Evol. 50, 523—533.

Martinón-Torres, M., Bermúdez de Castro, J.M., Gómez-Robles, A., Arsuaga, J.L., Carbonell, E., Lordkipanidze, D., Manzi, G., Margvelashvili, A., 2007. Dental evidence on the hominin dispersals during the Pleistocene. Proc. Natl. Acad. Sci. USA 104, 13279—13282.

Martinón-Torres, M., Bermúdez de Castro, J.M., Gómez-Robles, A., Margvelashvili, A., Prado, L., Lordkipanidze, D., Vekua, A., 2008. Dental remains from Dmanisi (Republic of Georgia): morphological analysis and comparative study. J. Hum. Evol. 55, 249—273.

Martinón-Torres, M., Bermúdez de Castro, J.M., Gómez-Robles, A., Prado-Simón, L., Arsuaga, J.L., 2012. Morphological description and comparison of the dental remains from Atapuerca-Sima de los Huesos site (Spain). J. Hum. Evol. 62, 7—58.

Martinón-Torres, M., Dennell, R., Bermúdez de Castro, J.M., 2011. The Denisova hominin need not be an out of Africa story. J. Hum. Evol. 60, 251—255.

McDougall, I., Brown, F.H., Fleagle, J., 2005. Stratigraphic placement and age of modern humans from Kibish, Ethiopia. Nature 433, 733—736.

Miller-Antonio, S., Schepartz, L., Karkanas, P., Hou, Y., Huang, W., Bekken, D., 2004. Lithic raw material use at the late Middle Pleistocene site of Panxian Dadong. Asian Perspect. 43, 314—332.

Mizoguchi, Y., 1985. Shovelling: a Statistical Analysis of Its Morphology. University of Tokyo Bulletin, 26. The University Museum, Tokyo. 1—52.

Molnar, S., 1971. Human tooth wear, tooth function and cultural variability. Am. J. Phys. Anthropol. 34, 175—190.

Paraso, C., Schepartz, L., Karkanas, P., Miller-Antonio, S., Wang, W., Huang, W., Si, X., Liu, J., Hou, Y., 2006. Paleoenvironment and site formation processes at Panxian Dadong. In: Decong, Y. (Ed.), Collected Works for the 40th Anniversary of Yuanmou Man Discovery and the International Conference on Paleoanthropological Studies. Yunnan Science & Technology Press, Kunming, China, pp. 302—316.

Quam, R.M., Arsuaga, J.L., Bermúdez de Castro, J.M., Díez, J.C., Lorenzo, C., Carretero, J.M., García, N., Ortega, A.I., 2001. Human remains from Valdegoba Cave (Huérmeces, Burgos, Spain). J. Hum. Evol. 41, 385—435.

Rabinovich, R., Hovers, E., 2004. Faunal analysis from Amud Cave: preliminary results and interpretations. Int. J. Osteoarchaeol. 14, 287—306.

Rightmire, P., 2008. *Homo* in the Middle Pleistocene: hypodigms, variation, and species recognition. Evol. Anthropol. 17, 8—21.

Rink, W.J., Schepartz, L.A., Miller-Antonio, S., Huang, W.W., Hou, Y., Bakken, D., Richter, D., Jones, H.L., 2003. Electron spin resonance (ESR) dating of mammalian tooth enamel at Panxian Dadong Cave, Guizhou, China. In: Shen, C., Keates, S. (Eds.), Current Research in Chinese Pleistocene Archaeology. BAR International Series, vol. 117, pp. 111—118.

Rohlf, F.J., 1998a. TpsRelw. Ecology and Evolution. SUNY, Stony Brook, New York. http://life.bio.sunysb.edu/morph/.

Rohlf, F., 1998b. TpsRegr. Ecology and Evolution. SUNY, Stony Brook, New York. http://life.bio.sunysb.edu/morph/.

Rohlf, F., 1998c. TpsDig. Ecology and Evolution. SUNY, Stony Brook, New York. http://life.bio.sunysb.edu/morph/.

Schepartz, L., Miller-Antonio, S. (Eds.), 2004. Asia and the middle pleistocene in global perspective. Asian Perspect. 43, 187—366.

Schepartz, L., Stoutamire, S., Bakken, D., 2001. Taphonomy of Stegodon orientalis at Panxian Dadong, a Middle Pleistocene site in Guizhou, south China. La Terra degli Elefanti (The world of Elephants). In: Proceedings of the 1st International Congress. Consiglio Nazionale delle Ricerche, Roma, pp. 243—246.

Schepartz, L., Stoutamire, S., Bakken, D., 2005. Stegodon orientalis from Panxian Dadong, a Middle Pleistocene archaeological site in Guizhou, south China: taphonomy, population structure and evidence for human interactions. Quatern. Int. 126—128, 271—282.

Schepartz, L., Miller-Antonio, S., 2010. Taphonomy, life history, and human exploitation of Rhinoceros sinensis at the middle Pleistocene site of Panxian Dadong, Guizhou, China. Int. J. Osteoarchaeol. 20, 253—268.

Scott, G.R., Turner II, C.G., 1997. The Anthropology of Modern Human Teeth: Dental Morphology and its Variation in Recent Human Populations. Cambridge University Press, Cambridge.

Shang, H., Tong, H., Zhang, S., Chen, F., Trinkaus, E., 2007. An early modern human from Tianyuan Cave, Zhoukoudian, China. Proc. Natl. Acad. Sci. USA 104, 6575—6578.

Sheets, H.D., 2001. Imp, Integrated Morphometric Package. http://www.canisius.edu/~sheets/morphsoft.html.

Shen, G., Liu, J., Jin, L., 1997. Preliminary results on U-series dating of Panxian Dadong in Guizhou Province, S-W China. Acta Anthropol. Sinica 16, 221—230.

Slice, D.E., 2005. Modern Morphometrics in Physical Anthropology. Plenum Press, New York.

Stiner, M., 1994. Honor Among Thieves: a Zooarchaeological Study of Neandertal Ecology. Princeton University Press, Princeton, NJ.

Stiner, M., 2004. A Comparison of photon densitometry and computed tomography parameters of bone density in ungulate body part profiles. J. Taphon. 2, 117—145.

Stringer, C.B., 1985. Middle Pleistocene hominid variability and the origin of Late Pleistocene humans. In: Delson, E. (Ed.), Ancestors: The Hard Evidence. Alan R. Liss, New York, pp. 289—296.

Tattersall, I., Schwartz, J.H., 2009. Evolution of the genus Homo. Ann. Rev. Earth Planet. Sci. 37, 67—92.

Thoma, A., Vallois, H.V., 1977. Les dents de l'Homme de Rabat. Bull. Mém. Soc. Anthropol. Paris 13, 31—58.

Tillier, A.M., 1979. La dentition de l'enfant mouste' rian Chateauneuf 2 de' couvert a` l'Abri de Hauteroche (Charente). L'Anthropologie 83, 417—438.

Tobias, P.V., 1991. Olduvai Gorge. In: The Skulls, Endocasts and Teeth of Homo habilis, vol. 4. Cambridge University Press, Cambridge.

Turner II, C.G., Nichol, C.R., Scott, G.R., 1991. Scoring procedures for key morphological traits of the permanent dentition: the Arizona State University dental anthropology system. In: Kelley, M., Larsen, C. (Eds.), Advances in Dental Anthropology. Wiley-Liss, New York, pp. 13—31.

Vallois, H.V., 1952. Les restes humains du gisement Mousterian de Monsempron. Ann. Paléontol. 38, 100—120.

Vandermeersch, B., 1981. Les Hommes Fossils de Qafzeh (Israel). Centre National de la Recherche Scientifique, Paris. 176—177.

Vlcek, E., 1969. Neandertaler der Tschechoslowakei. Verlag der Tschechoslowakischen Akademie der Wissenschaften, Prague.

Weidenreich, F., 1937. The dentition of Sinanthropus pekinensis: a comparative odontography of the hominids. The geological survey of China. Palaeontologica Sinica New Ser. D 1, 1—180.

White, T., Asfaw, B., DeGusta, D., Gilbert, H., Richards, G., Suwa, G., Howell, C., 2003. Pleistocene Homo sapiens from Middle Awash, Ethiopia. Nature 423, 742—747.

Wolpoff, M.H., 1971. Metric Trends in Hominid Dental Evolution. Studies in Anthropology, vol. 2. Case Western Reserve University, Cleveland, OH.

Wolpoff, M.H., 1979. The Krapina dental remains. Am. J. Phys. Anthropol. 50, 67—114.

Wood, B., Abbott, S.A., Uytterschaut, H.T., 1988. Analysis of the dental morphology of Plio-Pleistocene hominids IV. Mandibular postcanine root morphology. J. Anat. 156, 107—139.

Wood, B.A., Engleman, C.A., 1988. Analysis of the dental morphology of Plio-Pleistocene hominids V. Maxillary postcanine tooth morphology. J. Anat. 161, 1—35.

Wood, B.A., Uytterschaut, H., 1987. Analysis of the dental morphology of Plio-Pleistocene hominins III. Mandibular premolar crowns. J. Anat. 154, 121—156.

Wu, X.Z., Poirier, F.E., 1995. Human Evolution in China. Oxford University Press, Oxford.

Xing, S., Zhou, M., Liu, W., 2009. Crown morphology and variation of the lower premolars of Zhoukoudian Homo erectus. Chi. Sci. Bull. 54, 3905—3915.

Zelditch, M.L., Swiderski, D.L., Sheets, H.D., Fink, W.L., 2004. Geometric Morphometrics for Biologists: a Primer. Elsevier Academic Press, San Diego.